SUPPLEMENTARY FIGURES

Supplementary Figure 1 Participant flow and study design.

Supplementary Figure 2 Spearman's rank-order correlation between MD index and Healthy Food Diversity index.

Supplementary Figure 3 Daily intake of proteins, dietary fibre, total lipids, saturated fatty acids, monounsaturated fatty acids and polyunsaturated fatty acids from the food categories recorded by subjects in ConD and MedD group at baseline, 4w and 8w.

Supplementary Figure 4 Linear regression analysis used to test if the MD index significantly predicted Total Cholesterol reduction, after adjusting for age, gender, BMI and energy intake.

Supplementary Figure 5 Retention times and measured features of acylcarnitines.

Supplementary Figure 6. Identification of acyl carnitines comparing retention time and *m/z* measured in urine with retention times and *m/z* of authentic standards.

Supplementary Figure 7. Identification of isovalerylcarnitine comparing retention time and *m/z* measured in urine with retention time and *m/z* of an authentic standard.

Supplementary Figure 8. Identification of branched-chain amino acids comparing retention time and *m/z* measured in urine with retention time and *m/z* of authentic standards.

Supplementary Figure 9. Identification of aromatic amino acids comparing retention time and *m/z* measured in urine with retention time and *m/z* of authentic standards.

Supplementary Figure 10. Identification of dihydroxybenzoic acids comparing retention time and *m/z* measured in urine with retention times and *m/z* of authentic standards.

Supplementary Figure 11. Identification of Urolithin A and Urolithin A-glucuronide comparing retention times and *m/z* measured in urine with retention times and *m/z* of authentic standards.

Supplementary Figure 12. Identification of Urolithin C-glucuronide and Urolithin C comparing retention times and *m/z* measured in urine and faeces, respectively, with retention times and *m/z* of authentic standards.

Supplementary Figure 13. Identification of Tryptophan betaine comparing retention time, *m/z* and spectrum measured in urine with retention time, *m/z* and spectrum of an authentic standard.

Supplementary Figure 14. Identification of Oxindole-3-acetic acid comparing retention time, *m/z* and spectrum measured in urine with retention time, *m/z* and spectrum of an authentic standard.

Supplementary Figure 15. Identification of Pipecolic acid betaine comparing retention time and *m/z* measured in urine with retention time and *m/z* of an authentic standard.

Supplementary Figure 16. Identification of Phenyllactic acid comparing retention time and *m/z* measured in urine with retention time and *m/z* of an authentic standard.

Supplementary Figure 17. Identification of 3-methylpyrogallol-sulfate comparing retention time and *m/z* measured in urine with retention time and *m/z* of an authentic standard.

Supplementary Figure 18. Identification of Phenylacetylglutamine comparing retention time, *m/z* and spectrum measured in urine with retention time, *m/z* and spectrum of an authentic standard.

Supplementary Figure 19. Identification of P-cresol sulfate comparing retention time, *m/z* and spectrum measured in urine with retention time, *m/z* and spectrum of an authentic standard.

Supplementary Figure 20. Identification of Indoxyl sulfate comparing retention time, *m/z* and spectrum measured in serum with retention time, *m/z* and spectrum of an authentic standard. We noted a shift in retention time (0.3 min) for indoxyl sulfate compared to the original data collected.

Supplementary Figure 21. Identification of Phenol sulfate comparing retention time, *m/z* and spectrum measured in urine with retention time, *m/z* and spectrum of an authentic standard.

Supplementary Figure 22. Identification of 3-carboxy-4-methyl-5-propanyl-2-furanpropionic acid (CMPF) comparing retention time, *m/z* and spectrum measured in urine with retention time, *m/z* and spectrum of an authentic standard.

Supplementary Figure 23. Identification of trimethylamine-N-oxide (TMAO) comparing retention time and *m/z* measured in urine with retention time and *m/z* of an authentic standard.

Supplementary Figure 24. Retention times of bile acid authentic standards.

Supplementary Figure 25. Identification of Glycochenodeoxycholic acid sulfate comparing retention time and *m/z* measured in urine with retention time and *m/z* of an authentic standard.

Supplementary Figure 26 Diverging bar charts showing Spearman's correlations between MD Index and annotated metabolites from faecal, serum and urine metabolome.

Supplementary Figure 27 Barcoding plots of the contrasted MSP species between ConD and MedD diets at baseline.

Supplementary Figure 28 Barcoding plots of the contrasted MSP species between ConD and MedD diets at 4w.

Supplementary Figure 29 Barcoding plots of the contrasted MSP species between ConD and MedD diets at 8w.

Supplementary Figure 30 Distinctive metabolic, dietary and microbial signatures between ConD and MedD diets after 4 weeks.

Supplementary Figure 31 N-integrative supervised analysis of different types of 'omics datasets.

Supplementary Figure 32 Correlation of microbiome-related metabolites with dietary and clinical variables.

Supplementary Figure 33 Box plots showing faecal concentrations of several BAs measured throughout the intervention.

Supplementary Figure 34 Box plots showing differences in HOMA variation classifying the subjects in HOMA reducers and non-reducers after 4 weeks of intervention.

Supplementary Figure 35 Box plots showing differences in abundance of Co-Abundance Groups obtained from 16S rRNA gene sequences in subjects classified as HOMA reducers and non-reducers after 4 weeks of intervention.

Supplementary Figure 36 Circular tree showing clustering of the subjects based on *Faecalibacterium prausnitzii* pangenome.

SUPPLEMENTARY FIGURES

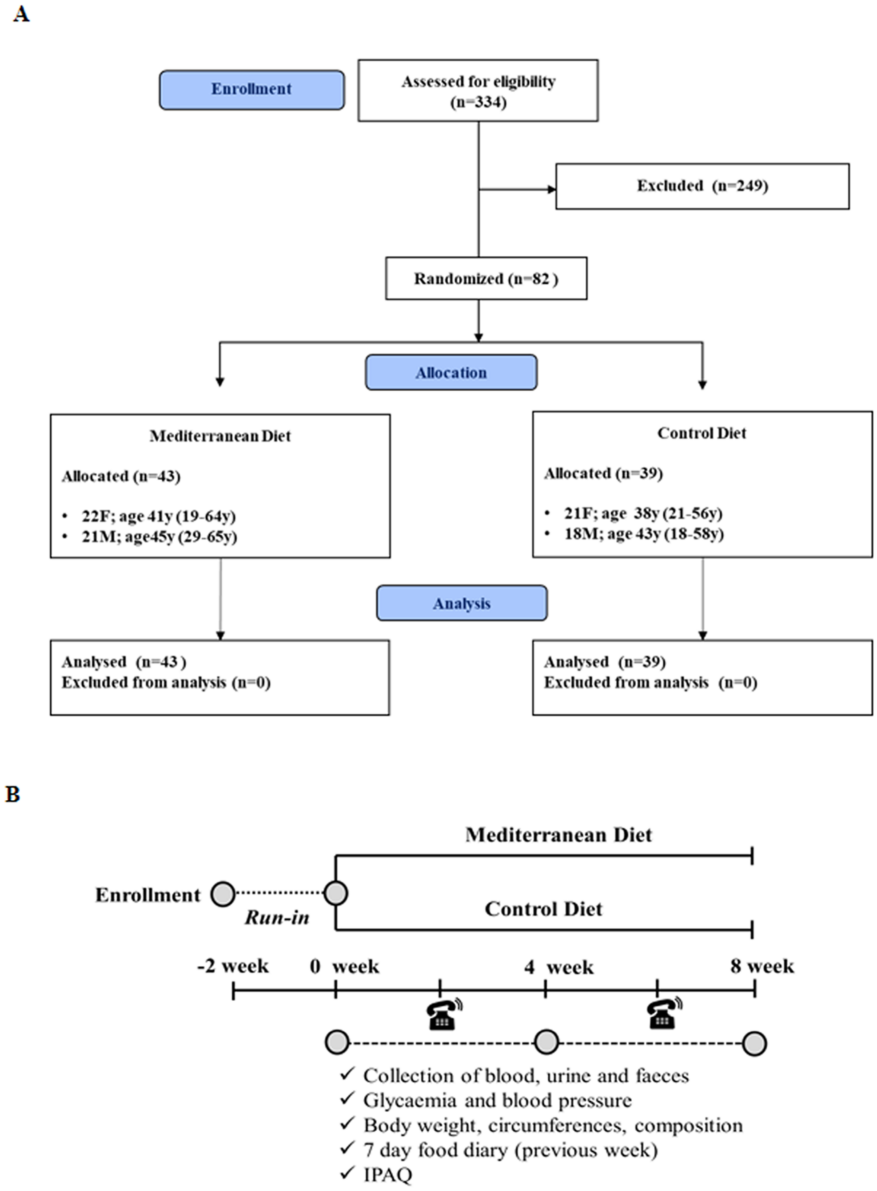

Supplementary Figure 1 (A) Participant flow and (B) study design.

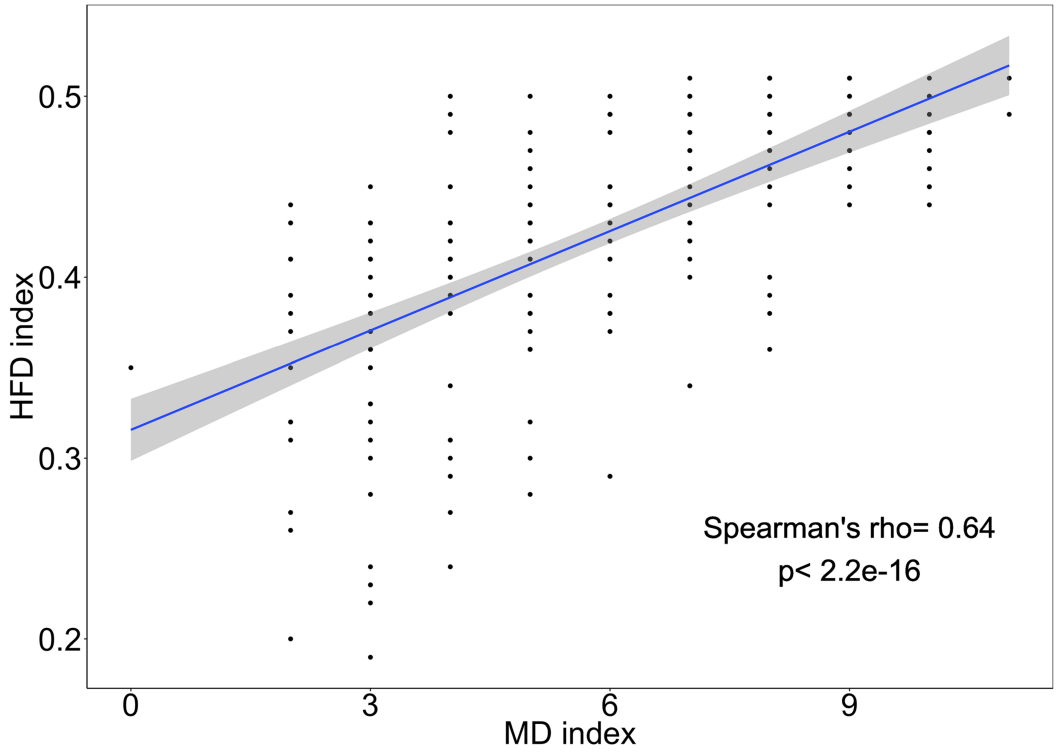

Supplementary Figure 2 Spearman's rank-order correlation between MD index and Healthy Food Diversity (HFD) index.

A

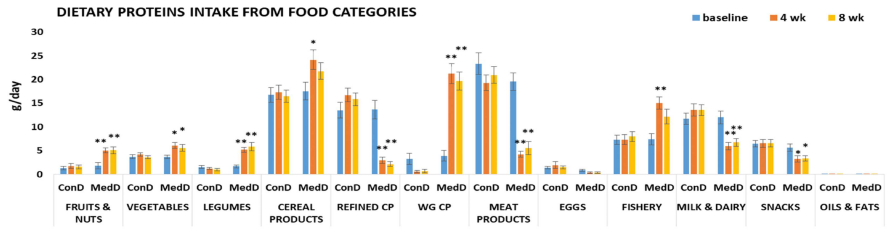
DIETARY PROTEINS INTAKE FROM FOOD CATEGORIES
baseline
4 wk
8 wk
g/day
ConD MedD
FRUITS & NUTS
VEGETABLES
LEGUMES
CEREAL PRODUCTS
REFINED CP
WG CP
MEAT PRODUCTS
EGGS
FISHERY
MILK & DAIRY
SNACKS
OILS & FATS

B

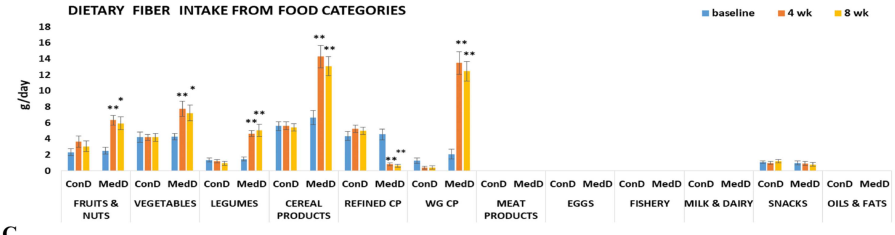
DIETARY FIBER INTAKE FROM FOOD CATEGORIES
baseline
4 wk
8 wk
g/day
ConD MedD
FRUITS & NUTS
VEGETABLES
LEGUMES
CEREAL PRODUCTS
REFINED CP
WG CP
MEAT PRODUCTS
EGGS
FISHERY
MILK & DAIRY
SNACKS
OILS & FATS

C

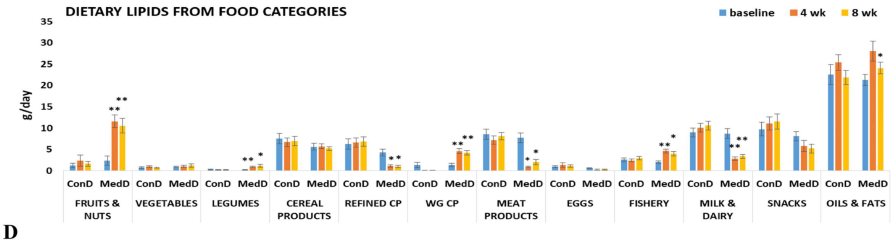
DIETARY LIPIDS FROM FOOD CATEGORIES
baseline
4 wk
8 wk
g/day
ConD MedD
FRUITS & NUTS
VEGETABLES
LEGUMES
CEREAL PRODUCTS
REFINED CP
WG CP
MEAT PRODUCTS
EGGS
FISHERY
MILK & DAIRY
SNACKS
OILS & FATS

D

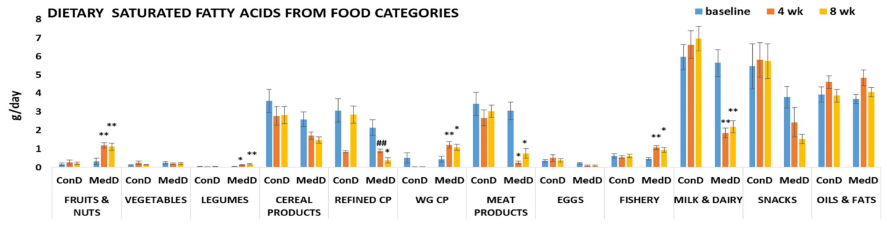
DIETARY SATURATED FATTY ACIDS FROM FOOD CATEGORIES
baseline
4 wk
8 wk
g/day
ConD MedD
FRUITS & NUTS
VEGETABLES
LEGUMES
CEREAL PRODUCTS
REFINED CP
WG CP
MEAT PRODUCTS
EGGS
FISHERY
MILK & DAIRY
SNACKS
OILS & FATS

E

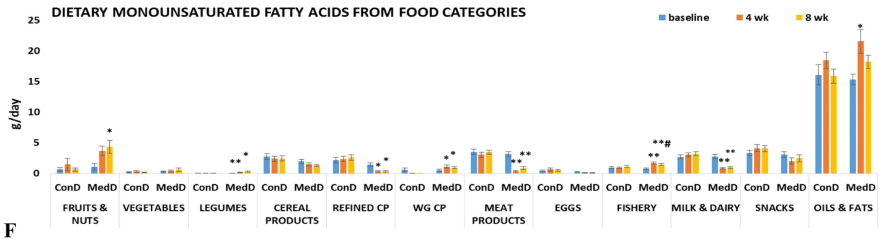
DIETARY MONOUNSATURATED FATTY ACIDS FROM FOOD CATEGORIES
baseline
4 wk
8 wk
g/day
ConD MedD
FRUITS & NUTS
VEGETABLES
LEGUMES
CEREAL PRODUCTS
REFINED CP
WG CP
MEAT PRODUCTS
EGGS
FISHERY
MILK & DAIRY
SNACKS
OILS & FATS

F

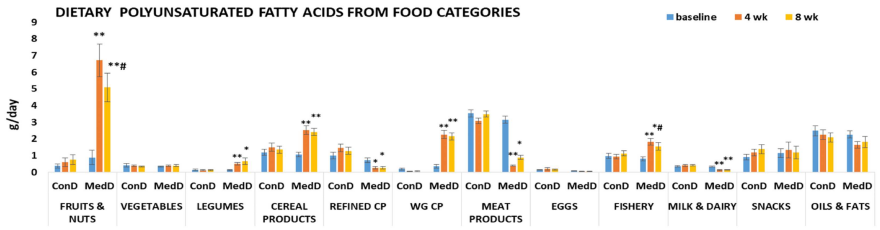
DIETARY POLYUNSATURATED FATTY ACIDS FROM FOOD CATEGORIES
baseline
4 wk
8 wk
g/day
ConD MedD
FRUITS & NUTS
VEGETABLES
LEGUMES
CEREAL PRODUCTS
REFINED CP
WG CP
MEAT PRODUCTS
EGGS
FISHERY
MILK & DAIRY
SNACKS
OILS & FATS

Supplementary Figure 3 Daily intake (g/day) of (A) proteins, (B) dietary fiber, (C) total lipids, (D) saturated fatty acids, (E) monounsaturated fatty acids and (F) polyunsaturated fatty acids from the food categories (fruits & nuts, vegetables, legumes, cereal products, refined cereal products, wholegrain-based cereal products, meat products, eggs, fishery, milk & dairy products, snacks, oil & fats) recorded by subjects in Control (ConD, n=32) and Mediterranean (MedD, n=30) diet group at baseline (week 0), 4w and 8w. Bars indicate the means±SEM. * indicates $p<0.05$ and ** indicates $p<0.001$ for MedD vs ConD at specific time point compared to baseline; # indicates $p<0.05$ and ## indicates $p<0.001$ for MedD vs ConD at 8w vs 4w; 2-way ANOVA with repeated measures and Tukey post hoc test.

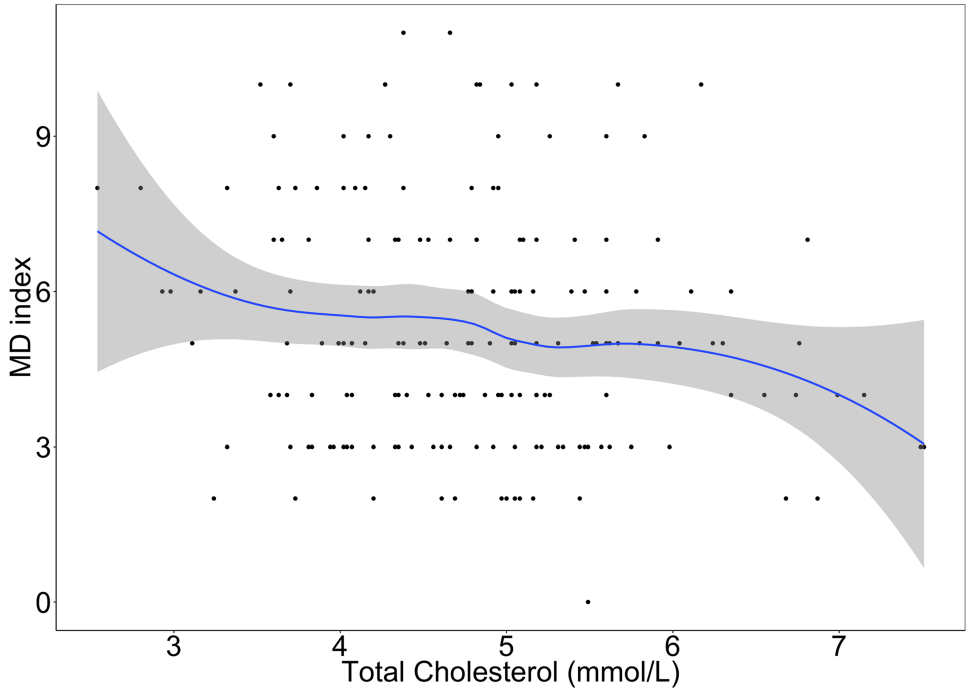

Supplementary Figure 4 Linear regression analysis used to test if the MD index significantly predicted Total Cholesterol reduction, after adjusting for age, gender, BMI and energy intake. The result of the regression indicated the predictors explained the 28% of the variance (Adjusted R-squared= 0.26, pvalue: 1.206e-11). Total Cholesterol (mmol/L) = 4.38 – 0.08 MD index.

Acylcarnitines

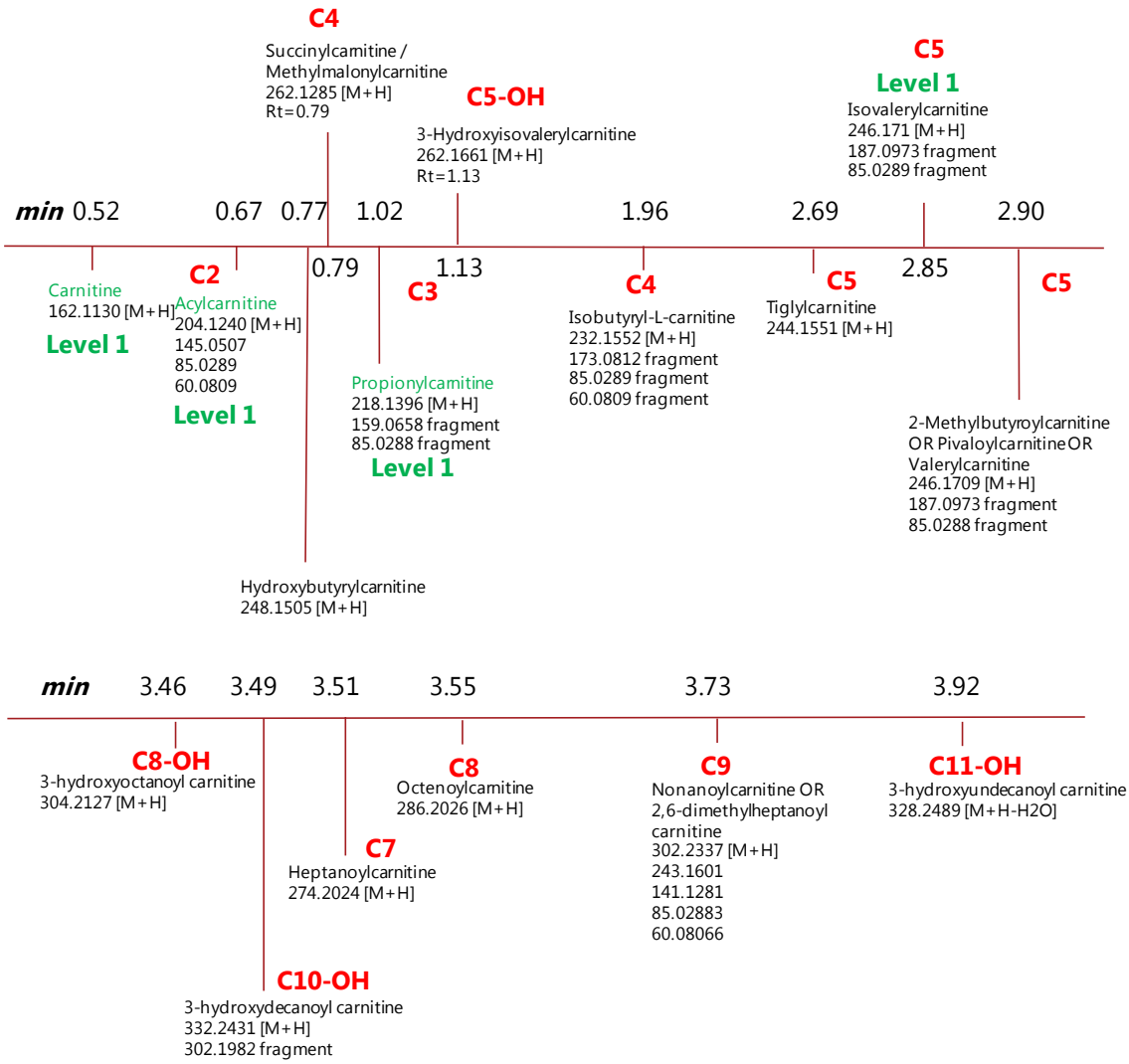

Supplementary Figure 5. Retention times and measured features of acylcarnitines. The acyl chain length is marked with the red letters from C2 to C11. Carnitine, acylcarnitine, propionylcarnitine and isovalerylcarnitine were validated using authentic standards (level 1 identification). The other acylcarnitines were identified at level 3.

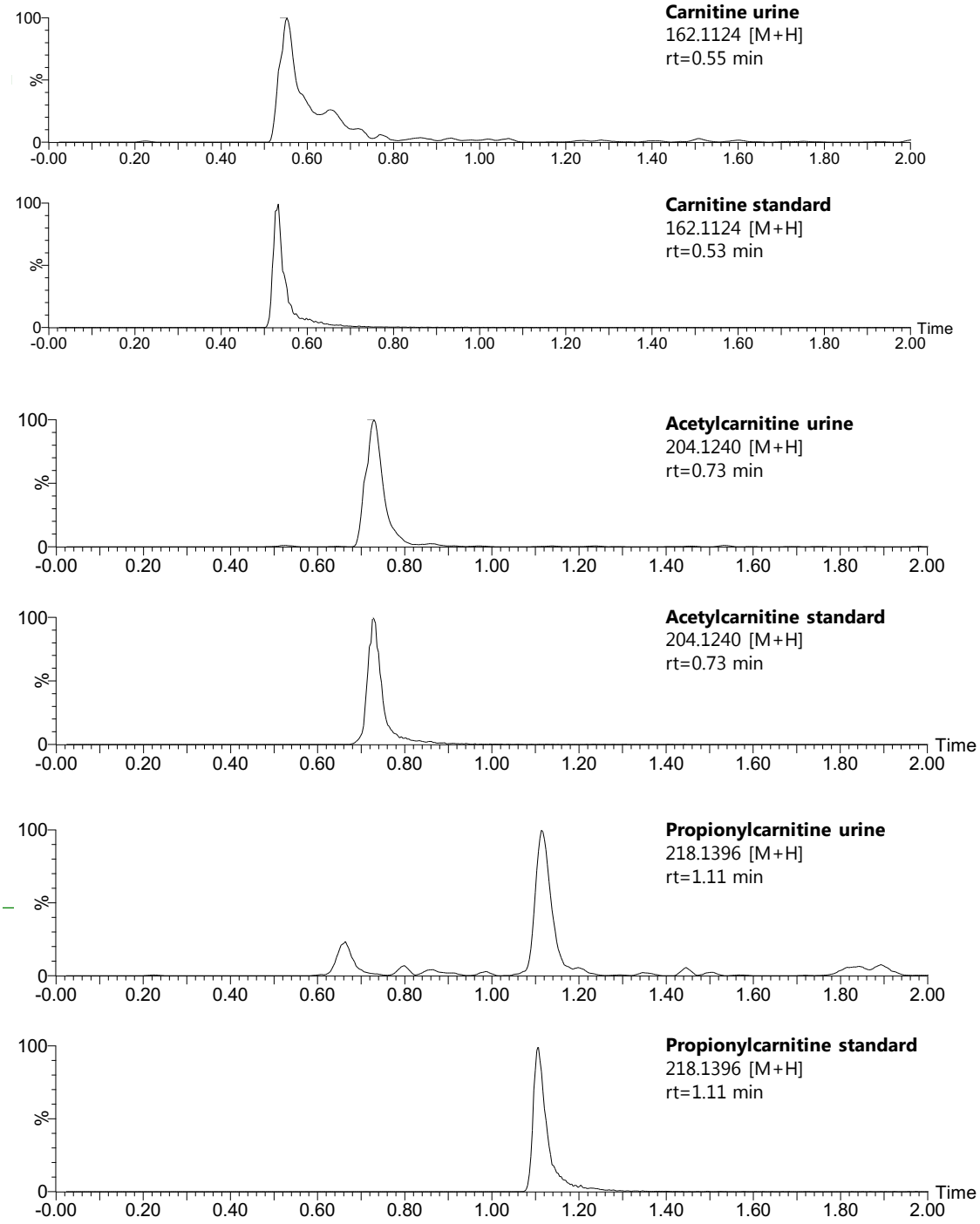

Supplementary Figure 6. Identification of acyl carnitines comparing retention time and *m/z* measured in urine with retention times and *m/z* of authentic standards.

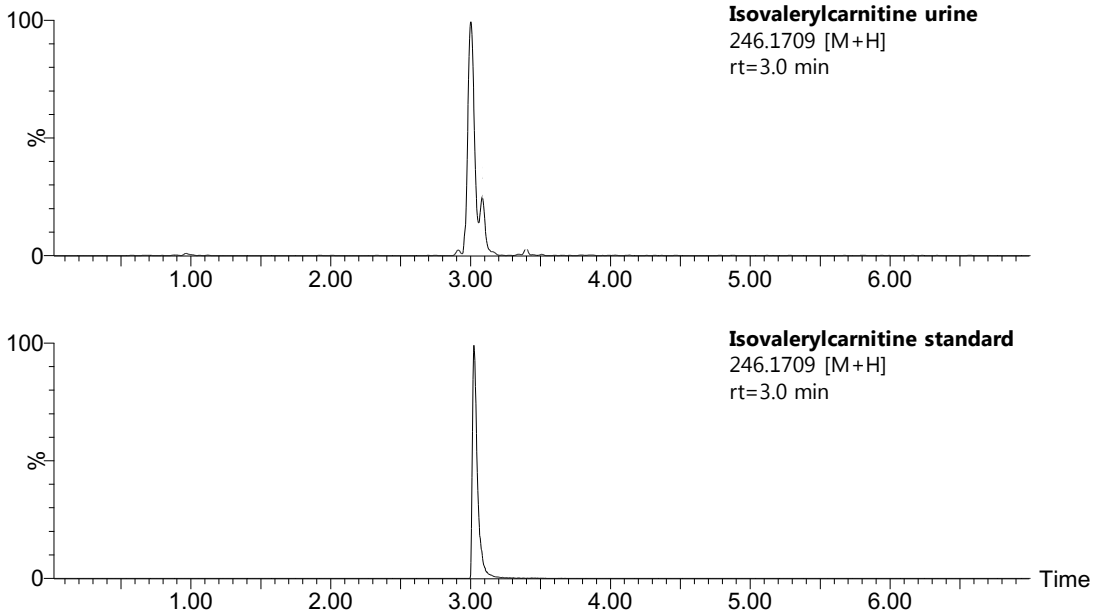

Supplementary Figure 7. Identification of isovalerylcarnitine comparing retention time and *m/z* measured in urine with retention time and *m/z* of an authentic standard.

Amino acids

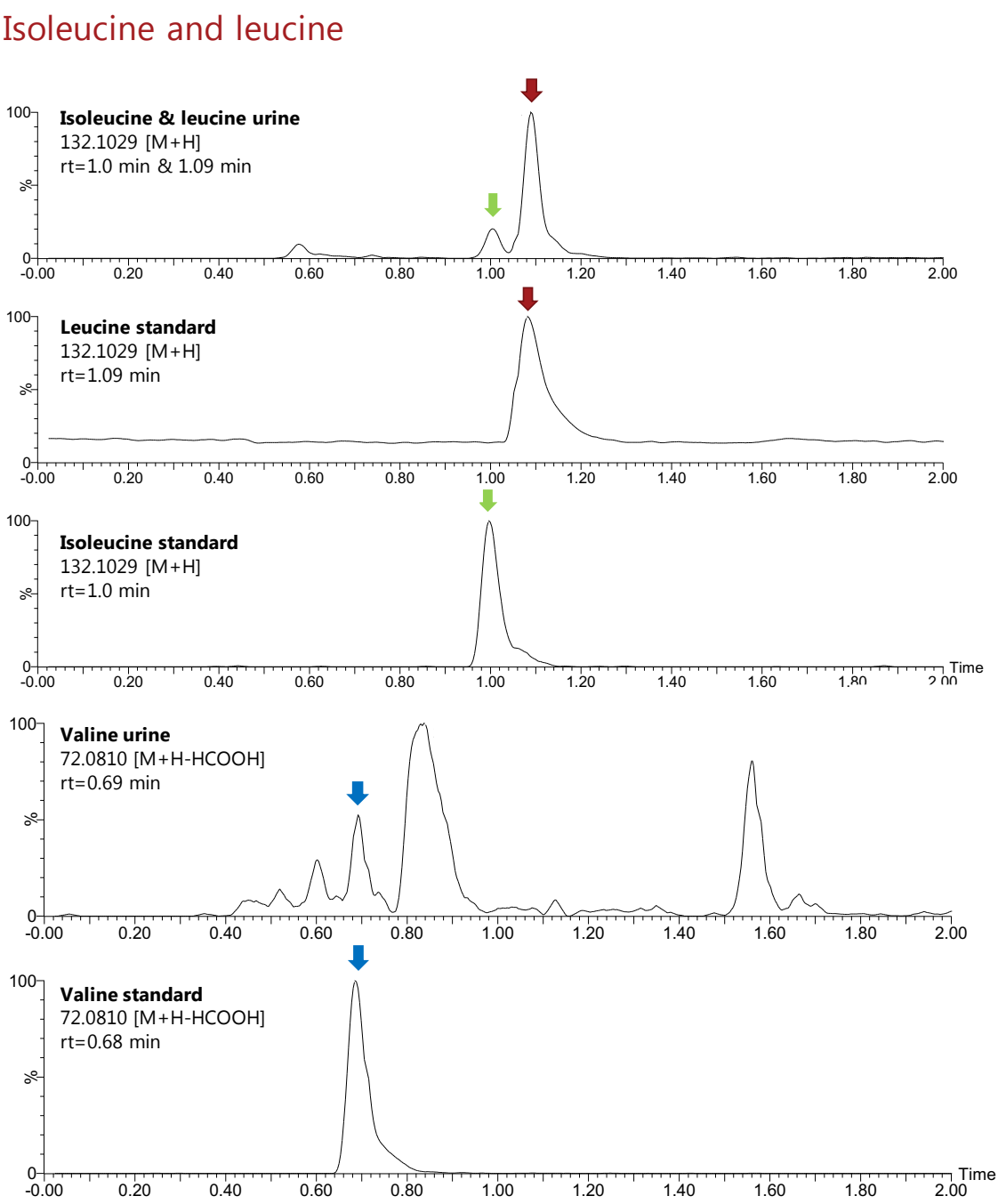

Supplementary Figure 8. Identification of branched-chain amino acids comparing retention time and *m/z* measured in urine with retention time and *m/z* of authentic standards.

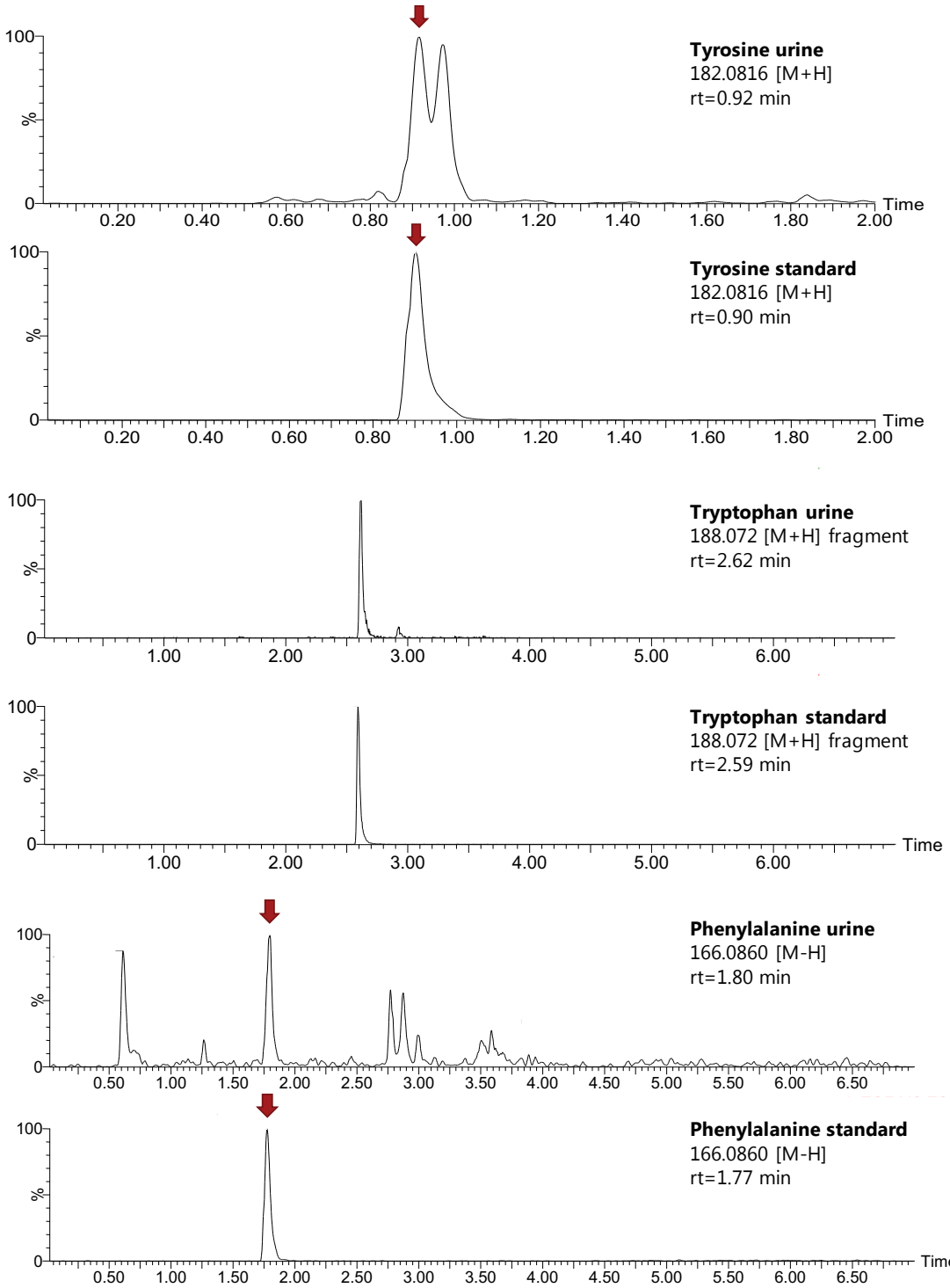

Supplementary Figure 9. Identification of aromatic amino acids comparing retention time and *m/z* measured in urine with retention time and *m/z* of authentic standards.

Plant biomarkers

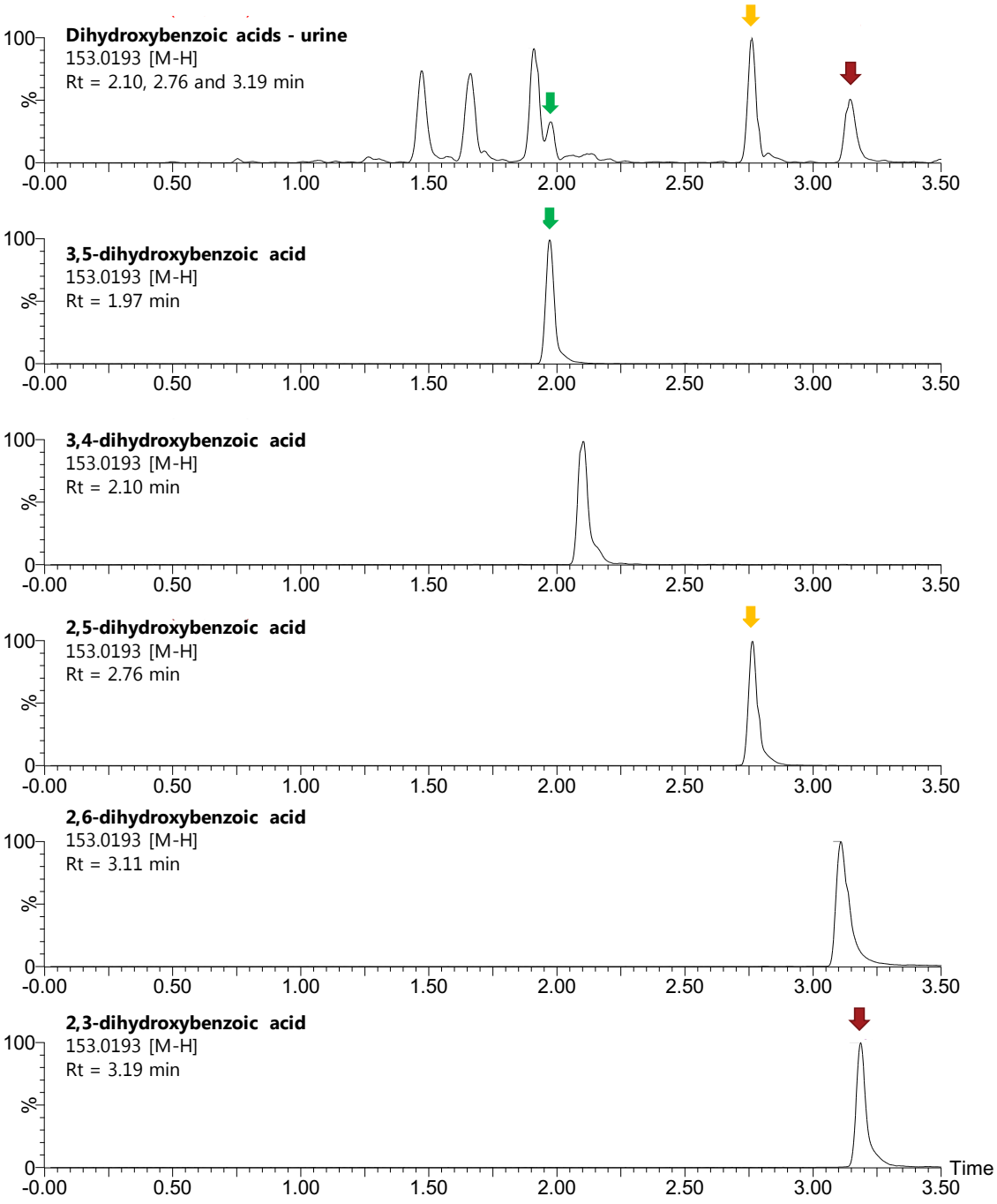

Supplementary Figure 10. Identification of dihydroxybenzoic acids comparing retention time and *m/z* measured in urine with retention times and *m/z* of authentic standards.

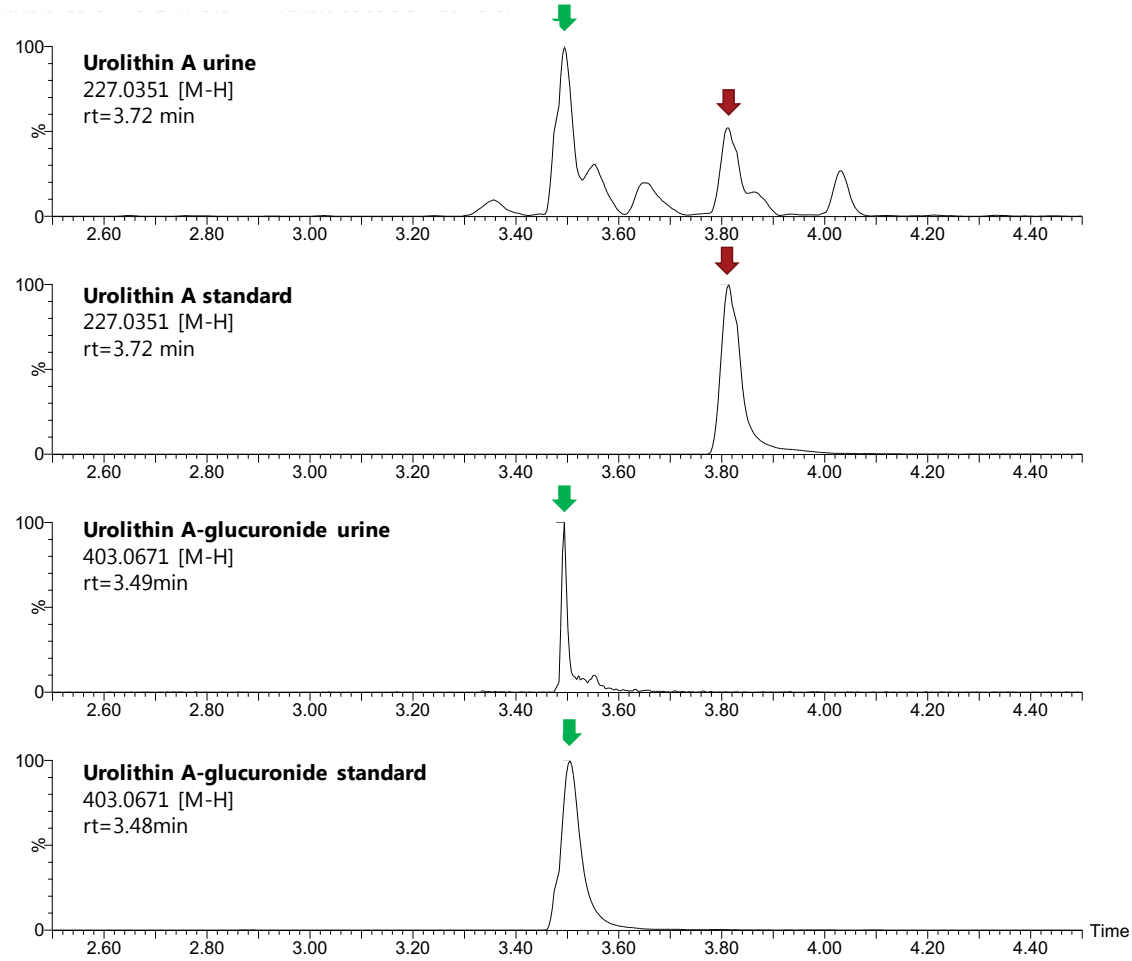

Supplementary Figure 11. Identification of Urolithin A and Urolithin A-glucuronide comparing retention times and *m/z* measured in urine with retention times and *m/z* of authentic standards.

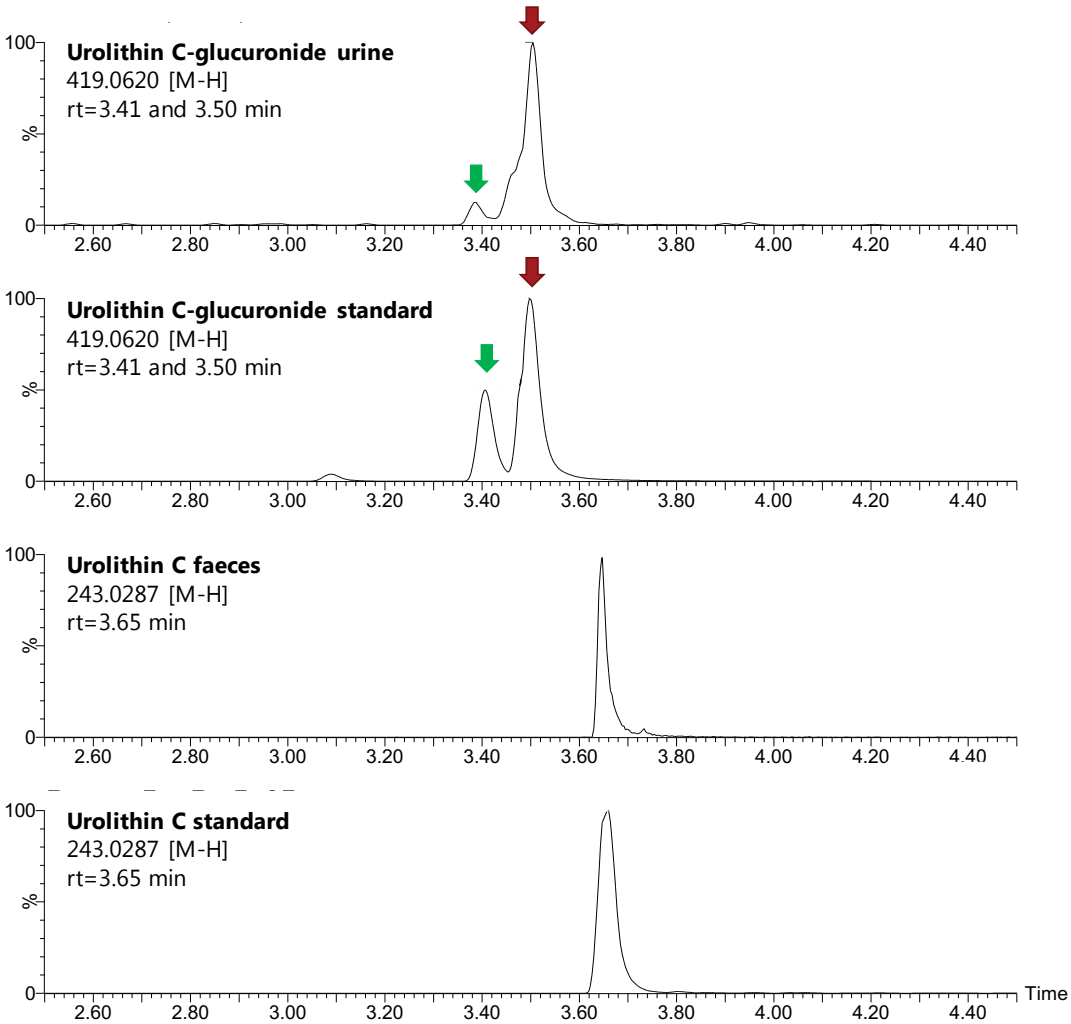

Supplementary Figure 12. Identification of Urolithin C-glucuronide and Urolithin C comparing retention times and *m/z* measured in urine and faeces, respectively, with retention times and *m/z* of authentic standards.

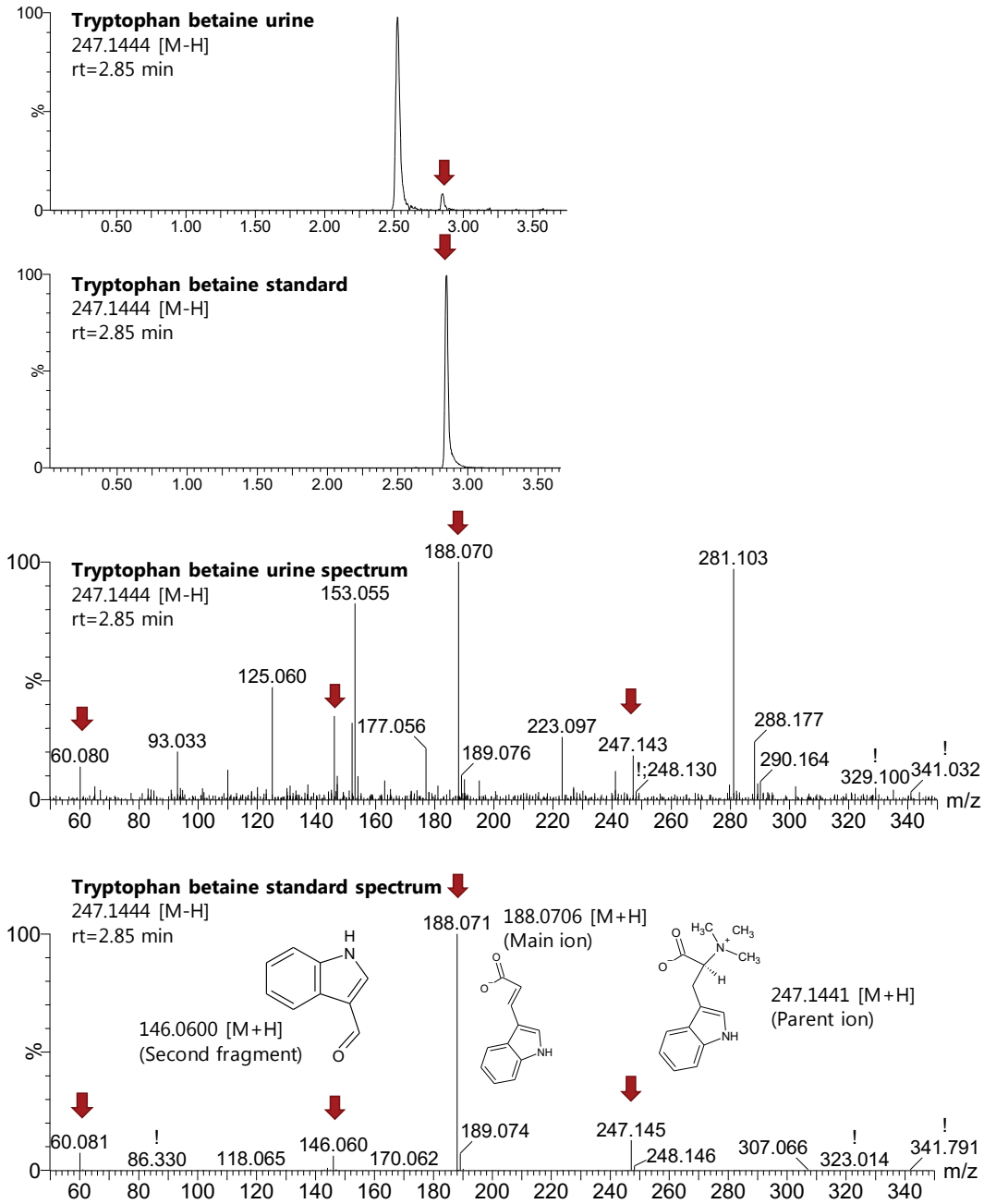

Supplementary Figure 13. Identification of Tryptophan betaine comparing retention time, *m/z* and spectrum measured in urine with retention time, *m/z* and spectrum of an authentic standard.

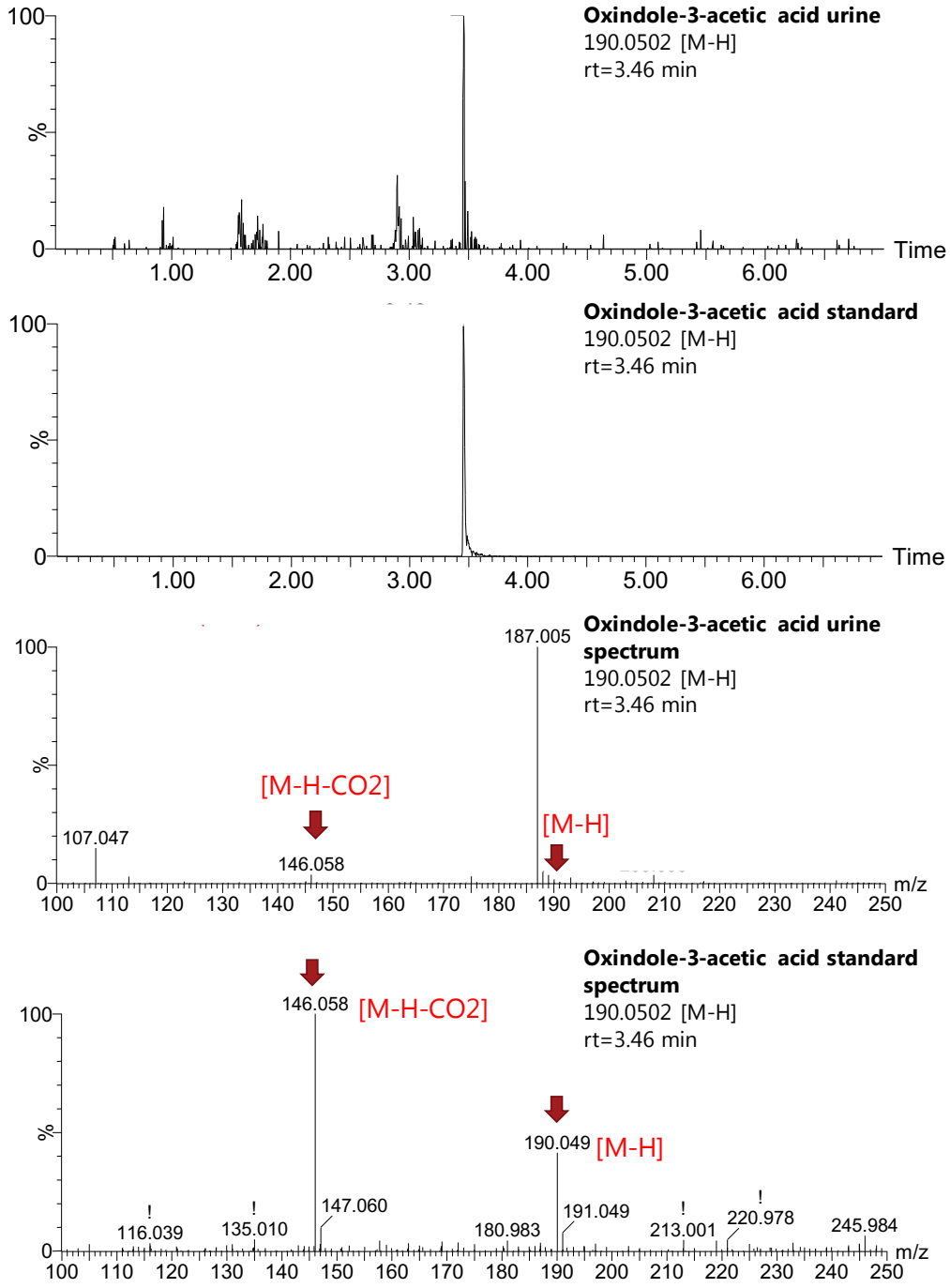

Supplementary Figure 14. Identification of Oxindole-3-acetic acid comparing retention time, *m/z* and spectrum measured in urine with retention time, *m/z* and spectrum of an authentic standard.

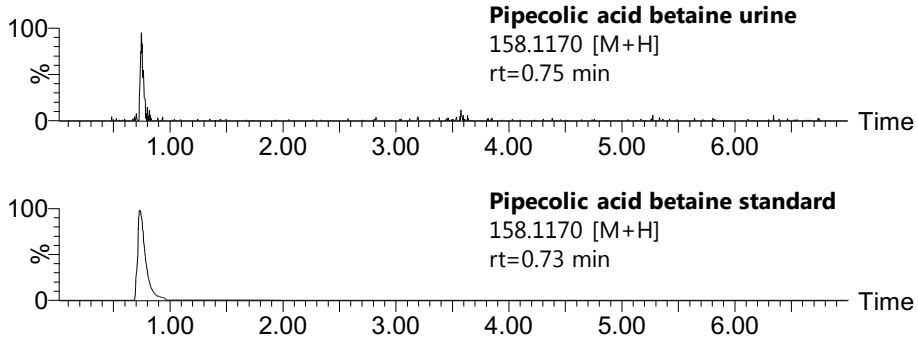

Supplementary Figure 15. Identification of Pipecolic acid betaine comparing retention time and *m/z* measured in urine with retention time and *m/z* of an authentic standard.

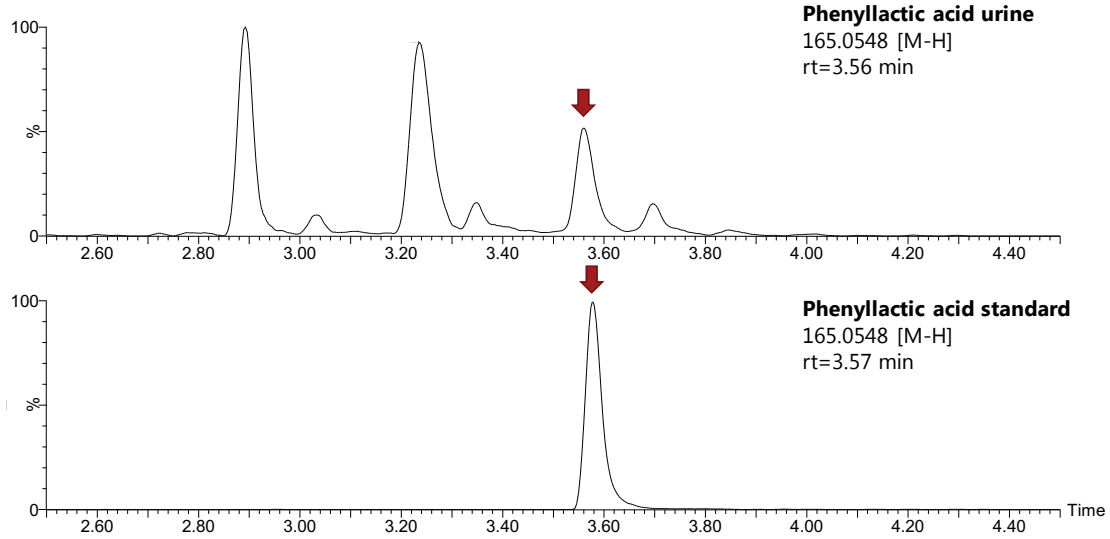

Supplementary Figure 16. Identification of Phenyllactic acid comparing retention time and *m/z* measured in urine with retention time and *m/z* of an authentic standard.

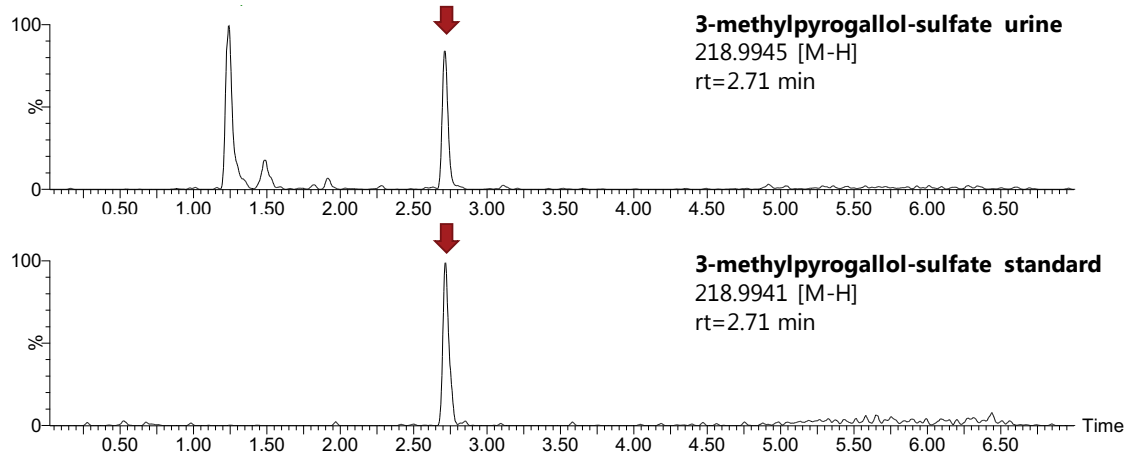

Supplementary Figure 17. Identification of 3-methylpyrogallol-sulfate comparing retention time and *m/z* measured in urine with retention time and *m/z* of an authentic standard.

Proteolytic degradation products

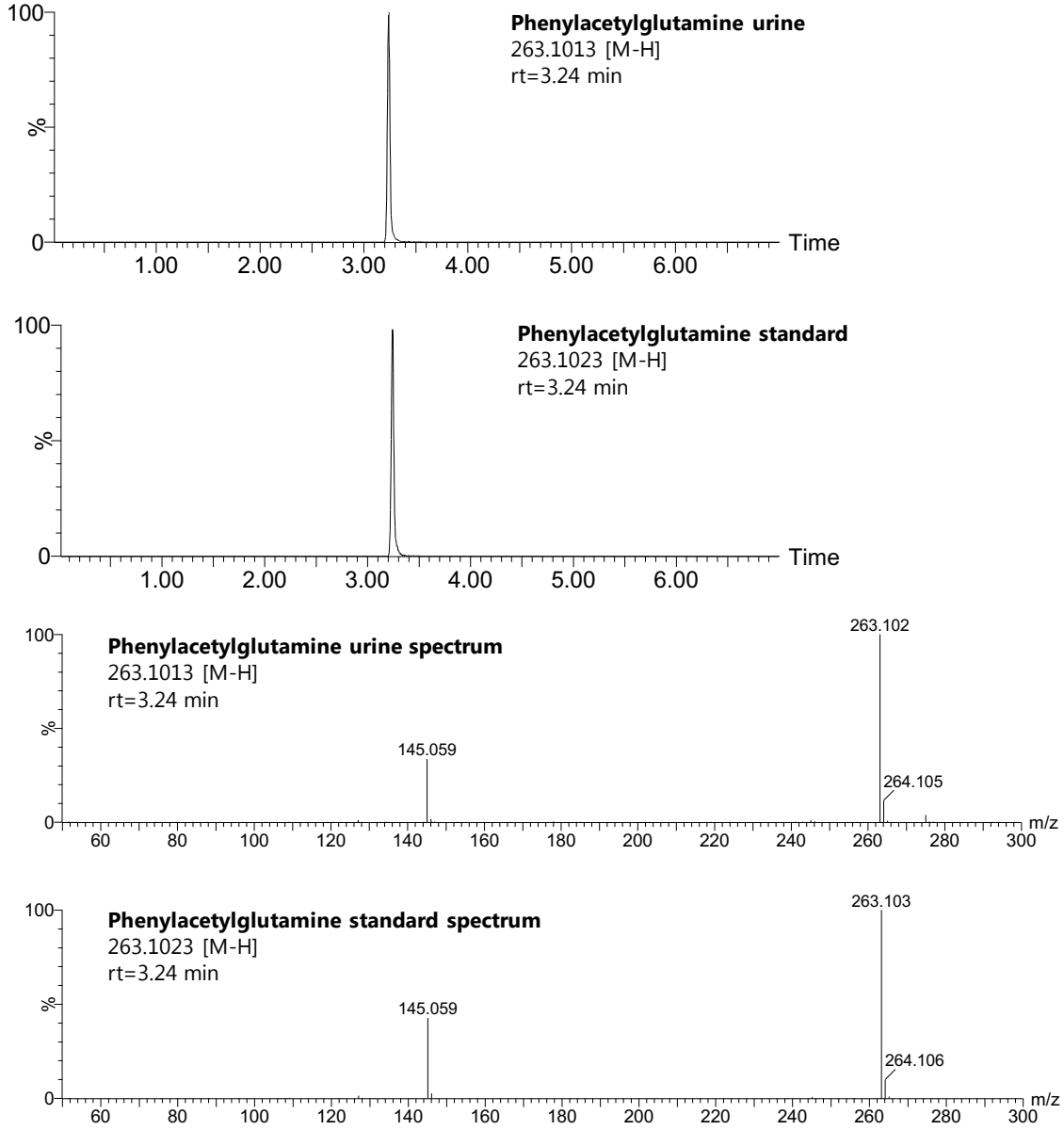

Supplementary Figure 18. Identification of Phenylacetylglutamine comparing retention time, *m/z* and spectrum measured in urine with retention time, *m/z* and spectrum of an authentic standard.

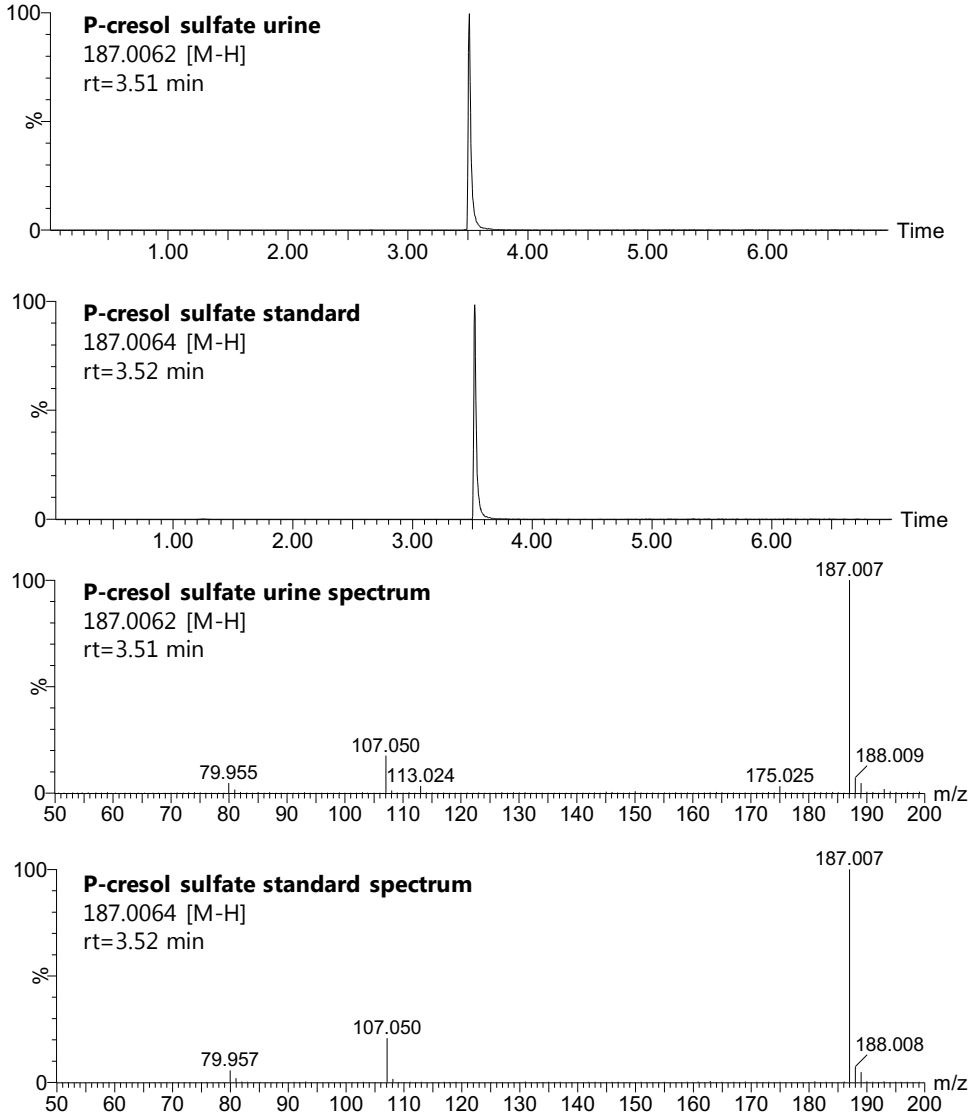

Supplementary Figure 19. Identification of P-cresol sulfate comparing retention time, *m/z* and spectrum measured in urine with retention time, *m/z* and spectrum of an authentic standard.

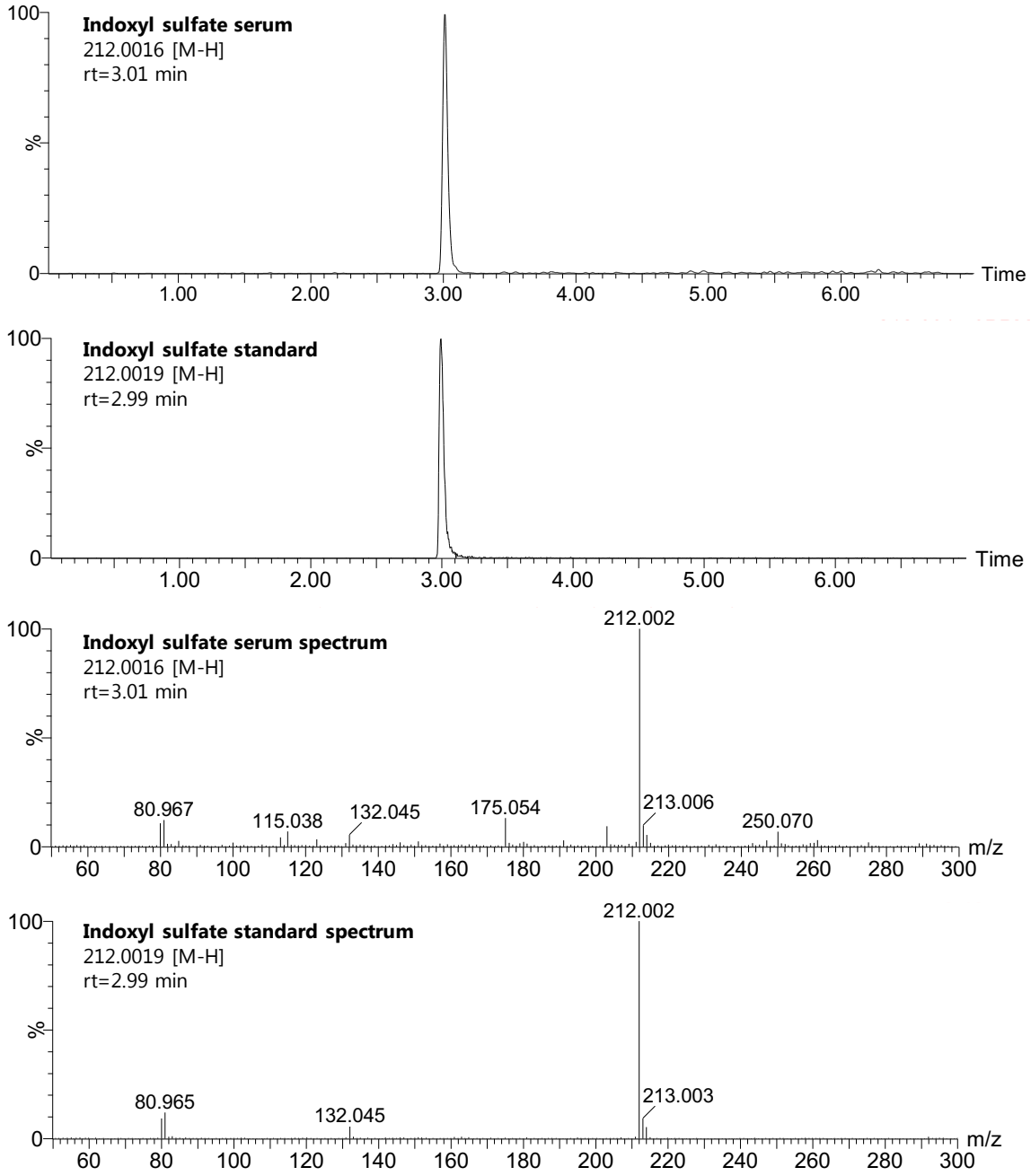

Supplementary Figure 20. Identification of Indoxyl sulfate comparing retention time, *m/z* and spectrum measured in serum with retention time, *m/z* and spectrum of an authentic standard. We noted a shift in retention time (0.3 min) for indoxyl sulfate compared to the original data collected.

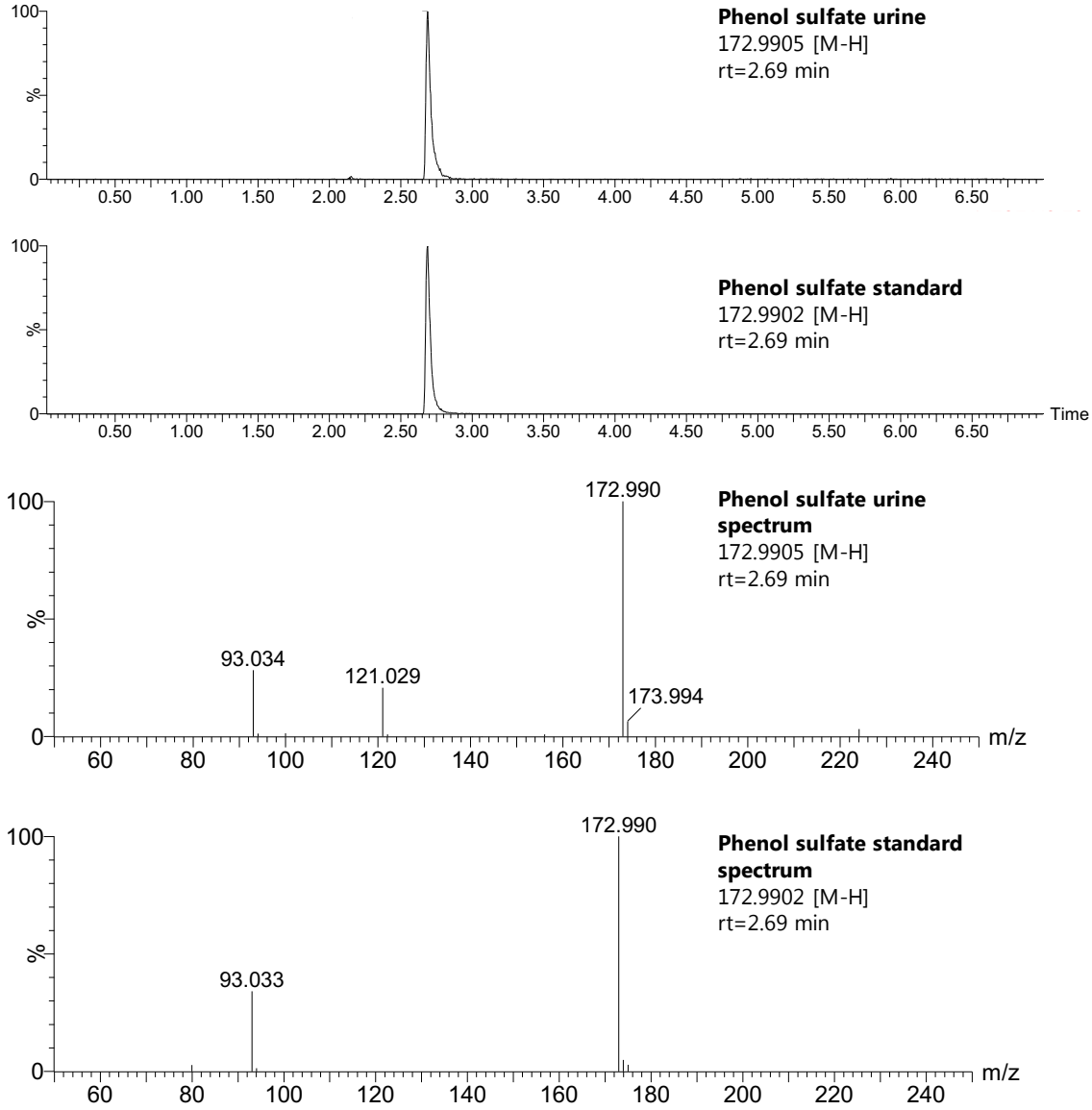

Supplementary Figure 21. Identification of Phenol sulfate comparing retention time, *m/z* and spectrum measured in urine with retention time, *m/z* and spectrum of an authentic standard.

Biomarkers of fish

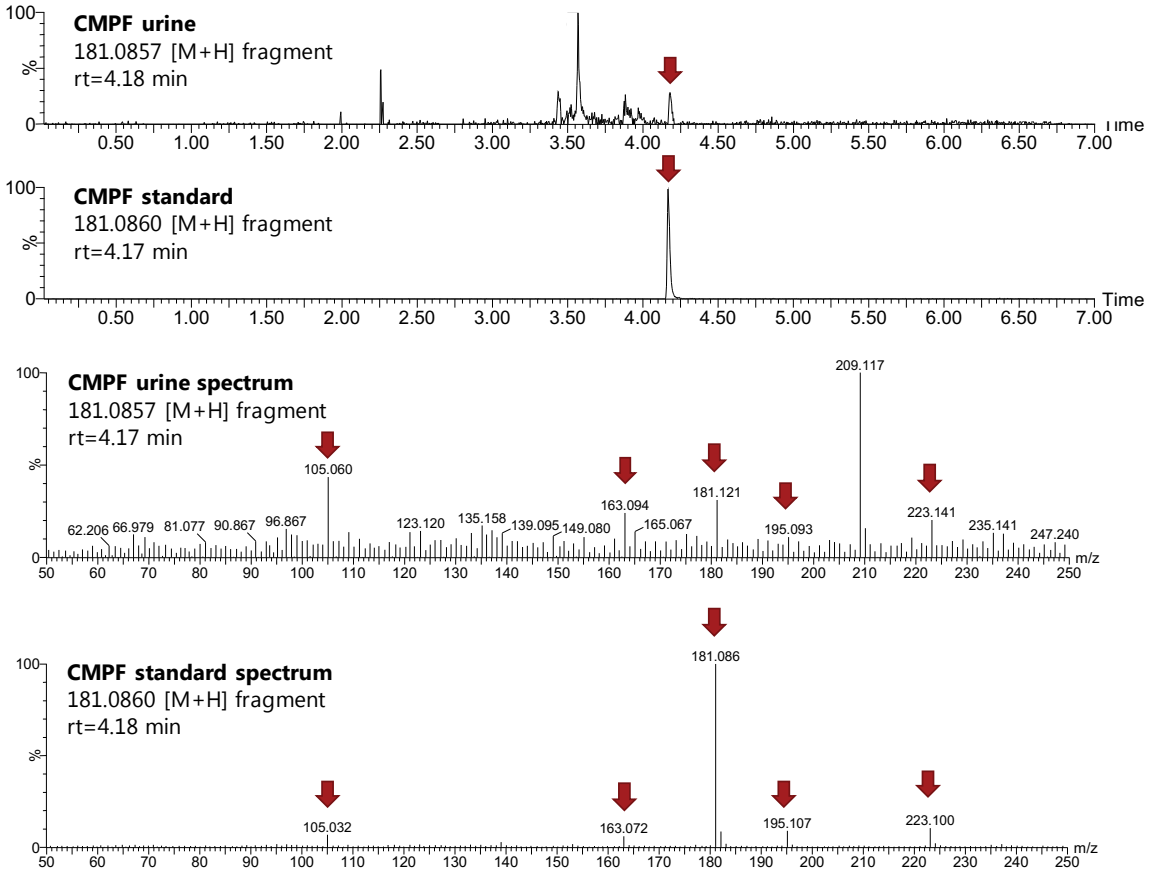

Supplementary Figure 22. Identification of 3-carboxy-4-methyl-5-propanyl-2-furanpropionic acid (CMPF) comparing retention time, *m/z* and spectrum measured in urine with retention time, *m/z* and spectrum of an authentic standard.

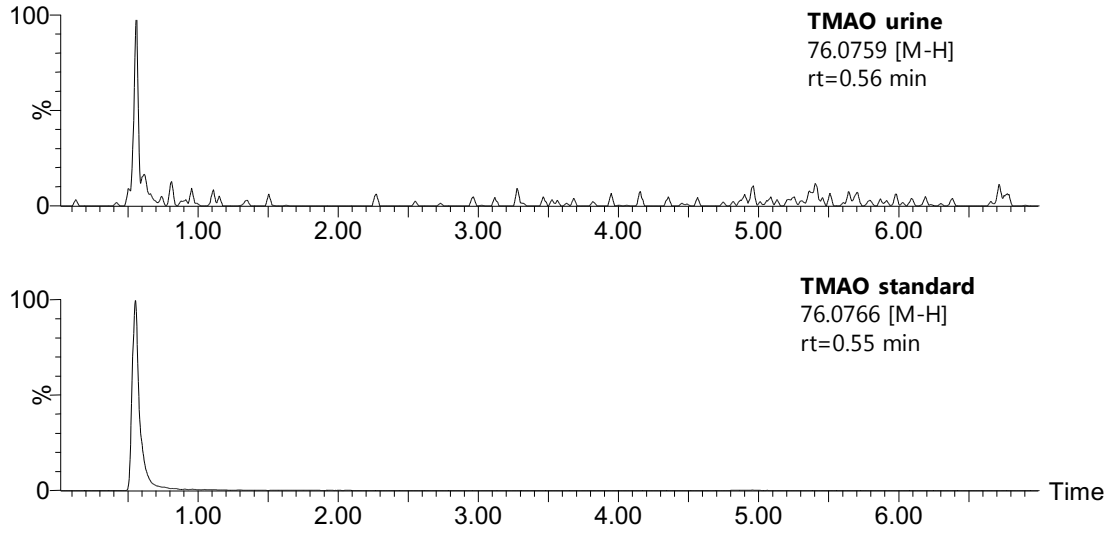

Supplementary Figure 23. Identification of trimethylamine-N-oxide (TMAO) comparing retention time and *m/z* measured in urine with retention time and *m/z* of an authentic standard.

Bile acids

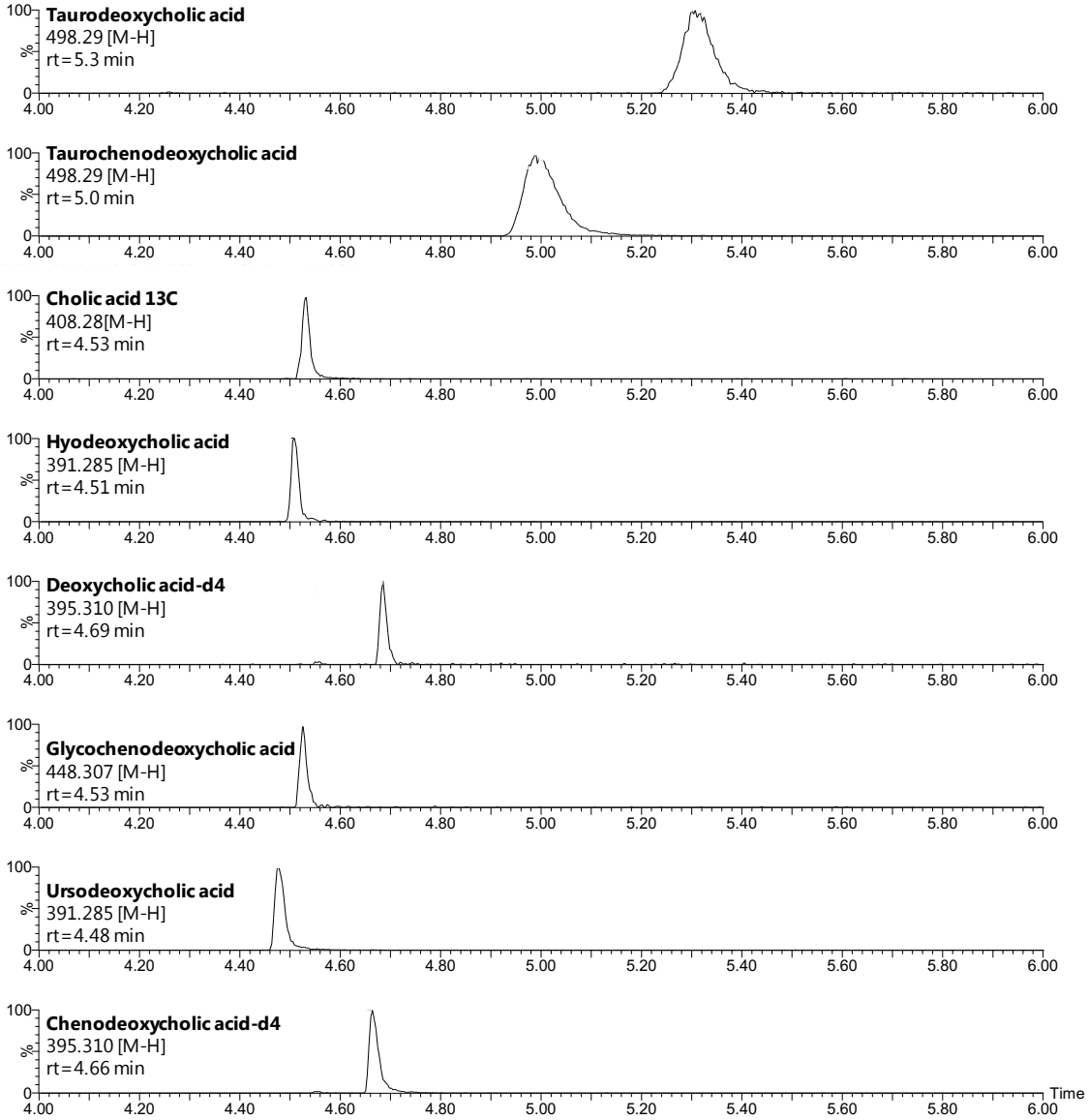

Supplementary Figure 24. Retention times of bile acid authentic standards.

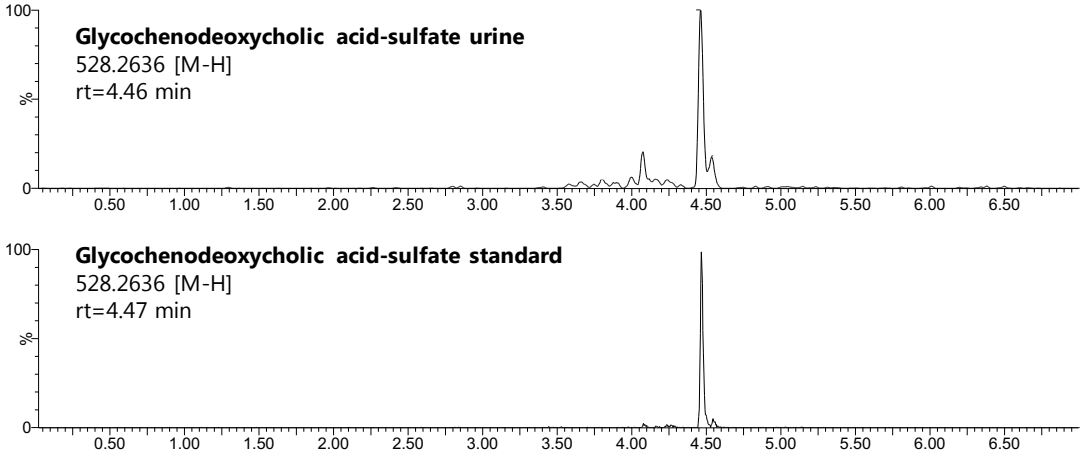

Supplementary Figure 25. Identification of Glycochenodeoxycholic acid sulfate comparing retention time and *m/z* measured in urine with retention time and *m/z* of an authentic standard.

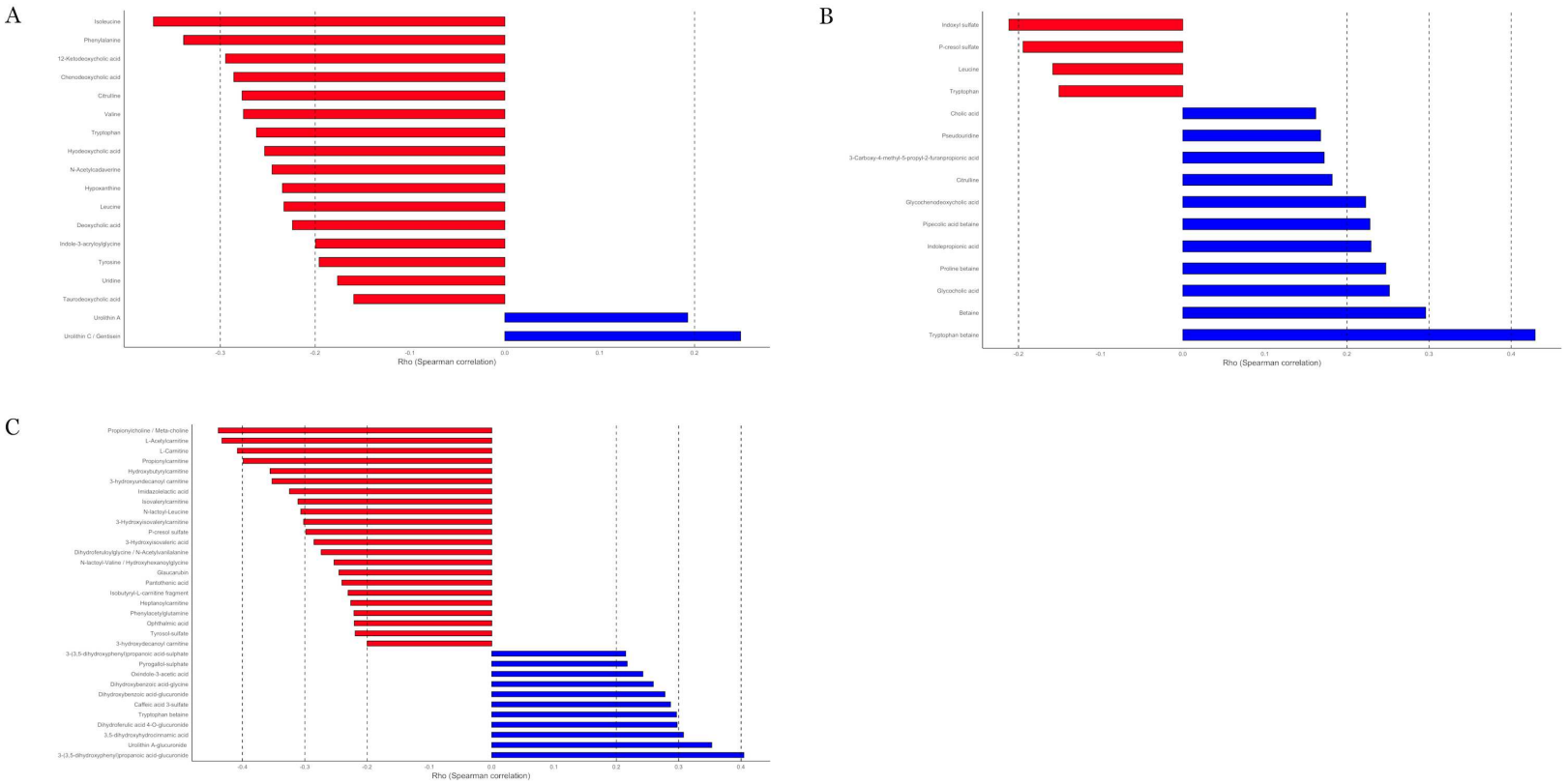

Supplementary Figure 26 Diverging bar charts showing Spearman's correlations between MD Index and annotated metabolites from (A) faecal, (B) serum and (C) urine metabolome. Red and blue horizontal bars indicate negative and positive correlations, respectively. Spearman's rho coefficients are displayed on the x-axis. (FDR<0.05).

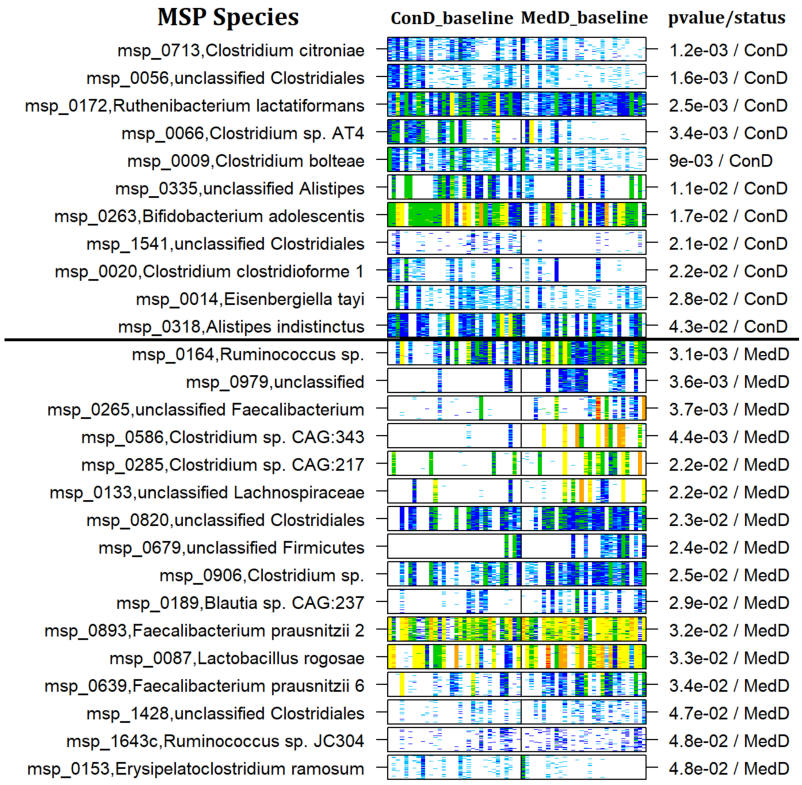

Supplementary Figure 27 Barcoding plots of the contrasted MSP species between ConD and MedD diets at baseline. Contrasted MSP species were computed using unpaired Wilcoxon rank sum tests on the MSP matrix filtered with a 20% occurrence threshold across samples. Contrasted MSP were organized in rows by blocks of their 50 marker genes and ranked by enrichment status (ConD or MedD) and by pvalues. Within each block, barcoding plots (heatmaps) of the frequency abundances of the marker genes were represented (white, absent; light blue to red, low to high abundance). Individuals were represented in columns by diet-time groups and ordered by their MSP richness at baseline.


MSP Species
ConD_4w
MedD_4w
pvalue/status
msp_0172 Ruthenibacterium lactatiformans 1.6e-04 / ConD
msp_0066 Clostridium sp. AT4 4.8e-03 / ConD
msp_0024 Hungatella hathewayi 2 5.6e-03 / ConD
msp_0249 unclassified Firmicutes 6.7e-03 / ConD
msp_0335 unclassified Alistipes 6.8e-03 / ConD
msp_0619 unclassified 8.9e-03 / ConD
msp_0058 Ruminococcus gnavus 9.4e-03 / ConD
msp_0707 unclassified Firmicutes 1.1e-02 / ConD
msp_0713 Clostridium citroniae 1.1e-02 / ConD
msp_0056 unclassified Clostridiales 1.3e-02 / ConD
msp_0052 Blautia sp. CAG:257 1.4e-02 / ConD
msp_0317 unclassified Clostridiales 1.4e-02 / ConD
msp_0331 Oscillibacter sp. 1.4e-02 / ConD
msp_0271 Eubacterium sp. CAG:180 1.4e-02 / ConD
msp_0126 Ruminococcus torques 1.5e-02 / ConD
msp_0621 Intestinibacter bartlettii 1.6e-02 / ConD
msp_0027 Parabacteroides merdae 1.6e-02 / ConD
msp_1090 unclassified 1.6e-02 / ConD
msp_0132 Coprobacillus cateniformis 1.7e-02 / ConD
msp_0318 Alistipes indistinctus 1.9e-02 / ConD
msp_0014 Eisenbergiella tayi 1.9e-02 / ConD
msp_0510 Clostridium glycyrrhizinilyticum 2.2e-02 / ConD
msp_1315 unclassified Firmicutes 2.7e-02 / ConD
msp_0364 Intestinimonas butyriciproducens 2.7e-02 / ConD
msp_0442 unclassified Flavonifractor 2.8e-02 / ConD
msp_0861 unclassified Oscillibacter 3.2e-02 / ConD
msp_0230 Allistipes inops 3.2e-02 / ConD
msp_1012 Intestinimonas massiliensis 3.3e-02 / ConD
msp_0833 Streptococcus thermophilus 3.3e-02 / ConD
msp_0522 Anaerotruncus colihominis 3.4e-02 / ConD
msp_0103 Clostridium innocuum 3.4e-02 / ConD
msp_0020 Clostridium clostridioforme 1 3.6e-02 / ConD
msp_0353 unclassified 4.2e-02 / ConD
msp_1541 unclassified Clostridiales 4.2e-02 / ConD
msp_1724 Phocea massiliensis 4.4e-02 / ConD
msp_0213 Flavonifractor plautii 4.5e-02 / ConD
msp_0881 Haemophilus parainfluenzae 9.1e-06 / MedD
msp_0388 Faecalibacterium prausnitzii 3 (L2-6) 9.8e-05 / MedD
msp_0884 Veillonella atypica 2.3e-04 / MedD
msp_1641 unclassified Lachnospiraceae 3.7e-04 / MedD
msp_1643c Ruminococcus sp. JC304 5.2e-04 / MedD
msp_0979 unclassified 1.6e-03 / MedD
msp_0906 Clostridium sp. 1.9e-03 / MedD
msp_0285 Clostridium sp. CAG:217 2.1e-03 / MedD
msp_0164 Ruminococcus sp. 2.4e-03 / MedD
msp_0313 Veillonella parvula 2.6e-03 / MedD
msp_0930 unclassified Lachnospiraceae 2.9e-03 / MedD
msp_1219 Veillonella rogosae 3e-03 / MedD
msp_0189 Blautia sp. CAG:237 3.7e-03 / MedD
msp_0265 unclassified Faecalibacterium 3.7e-03 / MedD
msp_0148c Veillonella dispar 5.8e-03 / MedD
msp_0457 Faecalibacterium sp. CAG:82 5.8e-03 / MedD
msp_0296 unclassified Lachnospiraceae 6.6e-03 / MedD
msp_0898 unclassified Firmicutes 6.7e-03 / MedD
msp_0468 unclassified Clostridiales 7.9e-03 / MedD
msp_0029 Eubacterium eligens 9.3e-03 / MedD
msp_0639 Faecalibacterium prausnitzii 6 9.4e-03 / MedD
msp_1236 unclassified Lachnoclostridium 1.1e-02 / MedD
msp_0301 Faecalibacterium prausnitzii 1 (A2-165) 1.1e-02 / MedD
msp_0075 Clostridium sp. 1.1e-02 / MedD
msp_0820 unclassified Clostridiales 1.4e-02 / MedD
msp_0473c Clostridium sp. 2.3e-02 / MedD
msp_0297 unclassified Ruminococcaceae 2.3e-02 / MedD
msp_0679 unclassified Firmicutes 2.4e-02 / MedD
msp_0572 Lachnospira sp. 2.5e-02 / MedD
msp_0015 Roseburia faecis 2.6e-02 / MedD
msp_0068 Eubacterium rectale 2.6e-02 / MedD
msp_0017 Roseburia intestinalis 2.6e-02 / MedD
msp_0563 unclassified Clostridium 3.2e-02 / MedD
msp_0125 unclassified Clostridiales 3.7e-02 / MedD
msp_1302 unclassified Firmicutes 3.9e-02 / MedD
msp_0986 Coprococcus catus 3.9e-02 / MedD
msp_0086 Clostridium symbiosum 4e-02 / MedD
msp_1143 unclassified Oscillibacter 4.1e-02 / MedD
msp_1339 Gordonibacter urolithinfaciens 4.2e-02 / MedD
msp_0227 Eubacterium sp. 36_13 & CAG:86 4.3e-02 / MedD
msp_0133 Coprococcus sp. 4.9e-02 / MedD

Supplementary Figure 28 Barcoding plots of the contrasted MSP species between ConD and MedD diets at 4w. Contrasted MSP species were computed using unpaired Wilcoxon rank sum tests on the MSP matrix filtered with a 20% occurrence threshold across samples. Contrasted MSP were organized in rows by blocks of their 50 marker genes and ranked by enrichment status (ConD or MedD) and by pvalues. Within each block, barcoding plots (heatmaps) of the frequency abundances of the marker genes were represented (white, absent; light blue to red, low to high abundance). Individuals were represented in columns by diet-time groups and ordered by their MSP richness at baseline.

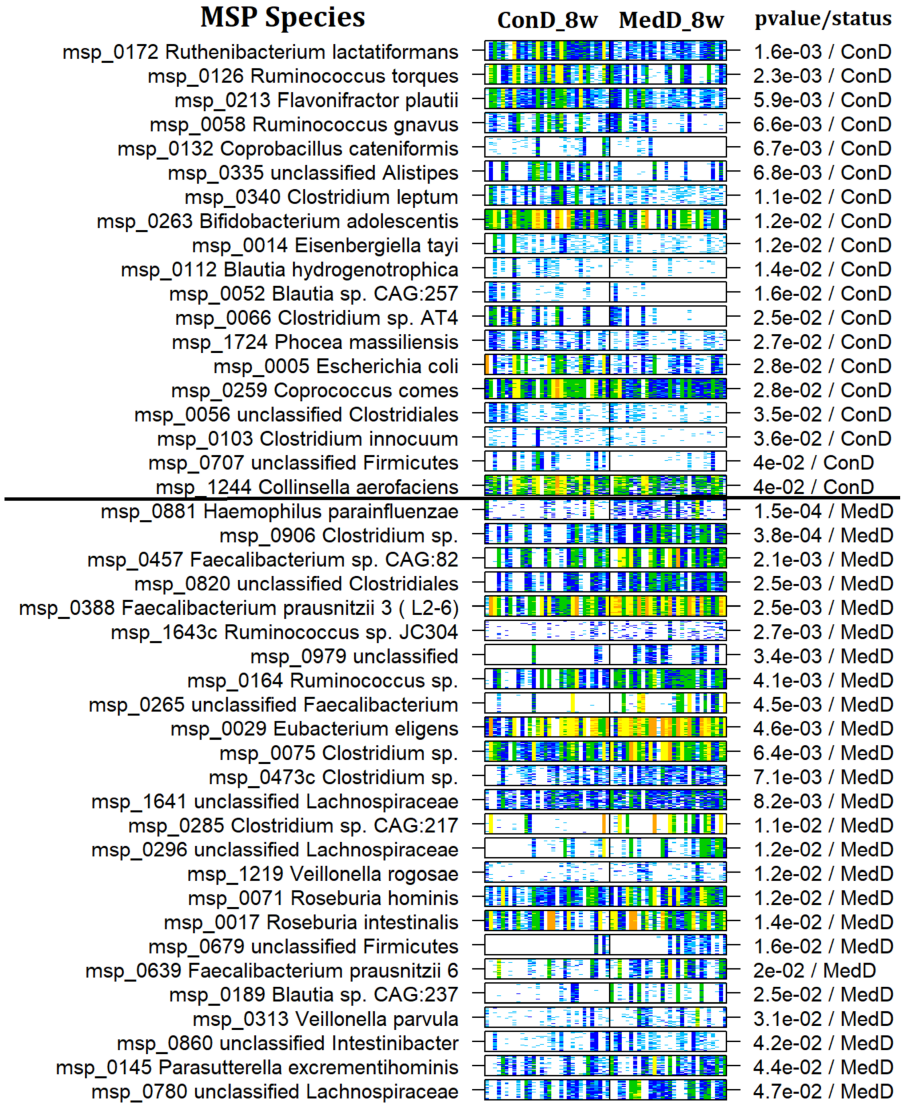

Supplementary Figure 29 Barcoding plots of the contrasted MSP species between ConD and MedD diets at 8w. Contrasted MSP species were computed using unpaired Wilcoxon rank sum tests on the MSP matrix filtered with a 20% occurrence threshold across samples. Contrasted MSP were organized in rows by blocks of their 50 marker genes and ranked by enrichment status (ConD or MedD) and by pvalues. Within each block, barcoding plots (heatmaps) of the frequency abundances of the marker genes were represented (white, absent; light blue to red, low to high abundance). Individuals were represented in columns by diet-time groups and ordered by their MSP richness at baseline.

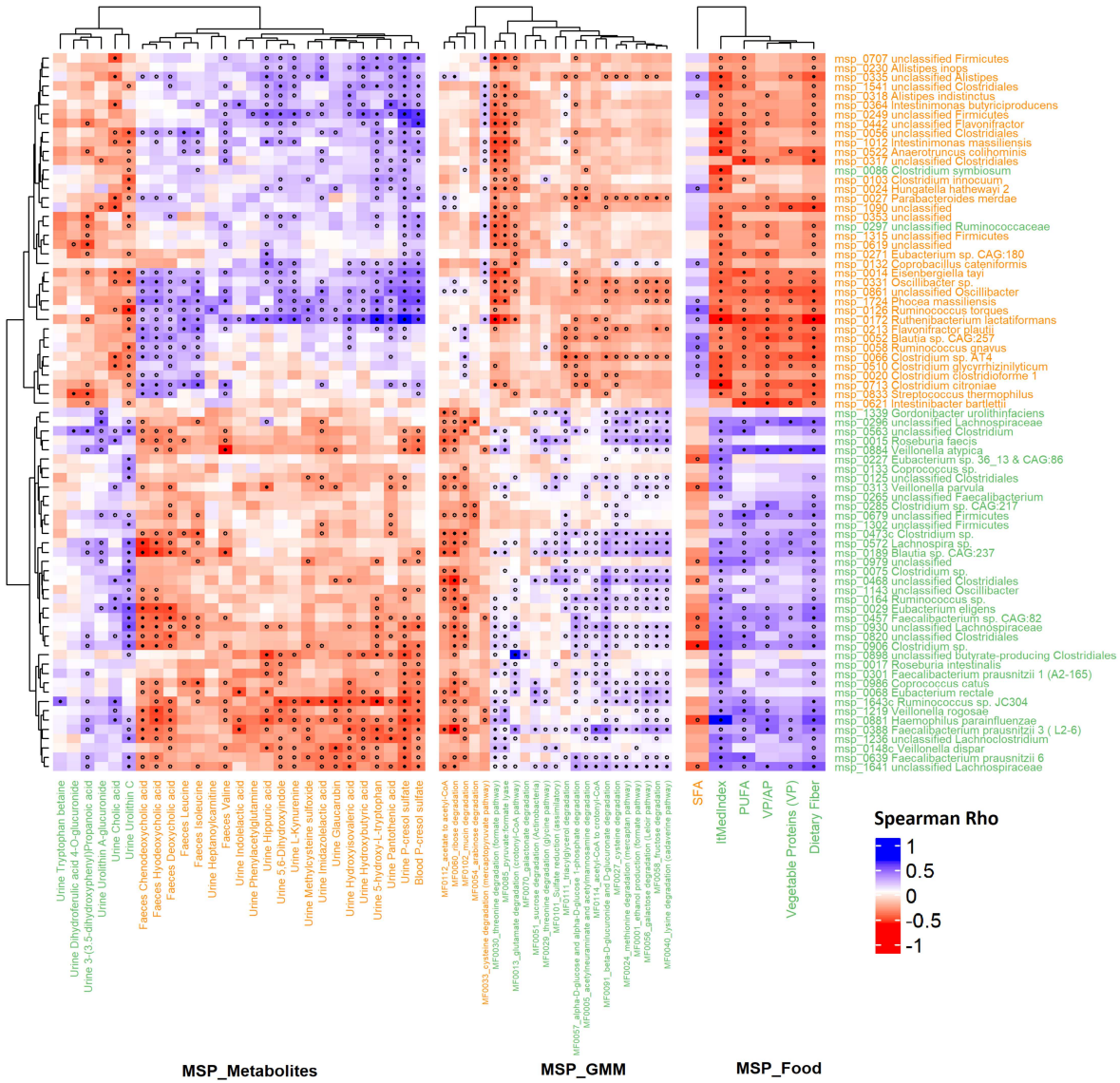
msp_0707 unclassified Firmicutes
msp_0230 Alistipes inops
msp_0335 unclassified Alistipes
msp_1541 unclassified Clostridiales
msp_0318 Alistipes indistinctus
msp_0364 Intestinimonas butyriciproducens
msp_0249 unclassified Firmicutes
msp_0442 unclassified Flavonifractor
msp_0056 unclassified Clostridiales
msp_1012 Intestinimonas massiliensis
msp_0522 Anaerotruncus colihominis
msp_0317 unclassified Clostridiales
msp_0086 Clostridium symbiosum
msp_0103 Clostridium innocuum
msp_0024 Hungatella hathewayi 2
msp_0027 Parabacteroides merdae
msp_1090 unclassified
msp_0353 unclassified
msp_0297 unclassified Ruminococcaceae
msp_1315 unclassified Firmicutes
msp_0619 unclassified
msp_0271 Eubacterium sp. CAG:180
msp_0132 Coprobacillus cateniformis
msp_0014 Eisenbergiella tayi
msp_0331 Oscillibacter sp.
msp_0861 unclassified Oscillibacter
msp_1724 Phocea massiliensis
msp_0126 Ruminococcus torques
msp_0172 Ruthenibacterium lactatiformans
msp_0213 Flavonifractor plautii
msp_0052 Blautia sp. CAG:257
msp_0058 Ruminococcus gnavus
msp_0066 Clostridium sp. AT4
msp_0510 Clostridium glycyrrhizinilyticum
msp_0020 Clostridium clostridioforme 1
msp_0713 Clostridium citroniae
msp_0833 Streptococcus thermophilus
msp_0621 Intestinibacter bartlettii
msp_1339 Gordonibacter urolithinfaciens
msp_0296 unclassified Lachnospiraceae
msp_0563 unclassified Clostridium
msp_0015 Roseburia faecis
msp_0884 Veillonella atypica
msp_0227 Eubacterium sp. 36_13 & CAG:86
msp_0133 Coprococcus sp.
msp_0125 unclassified Clostridiales
msp_0313 Veillonella parvula
msp_0265 unclassified Faecalibacterium
msp_0285 Clostridium sp. CAG:217
msp_0679 unclassified Firmicutes
msp_1302 unclassified Firmicutes
msp_0473c Clostridium sp.
msp_0572 Lachnospira sp.
msp_0189 Blautia sp. CAG:237
msp_0979 unclassified
msp_0075 Clostridium sp.
msp_0468 unclassified Clostridiales
msp_1143 unclassified Oscillibacter
msp_0164 Ruminococcus sp.
msp_0029 Eubacterium eligens
msp_0457 Faecalibacterium sp. CAG:82
msp_0930 unclassified Lachnospiraceae
msp_0820 unclassified Clostridiales
msp_0906 Clostridium sp.
msp_0898 unclassified butyrate-producing Clostridiales
msp_0017 Roseburia intestinalis
msp_0301 Faecalibacterium prausnitzii 1 (A2-165)
msp_0986 Coprococcus catus
msp_0068 Eubacterium rectale
msp_1643c Ruminococcus sp. JC304
msp_1219 Veillonella rogosae
msp_0881 Haemophilus parainfluenzae
msp_0388 Faecalibacterium prausnitzii 3 (L2-6)
msp_1236 unclassified Lachnoclostridium
msp_0148c Veillonella dispar
msp_0639 Faecalibacterium prausnitzii 6
msp_1641 unclassified Lachnospiraceae
Urine Tryptophan betaine
Urine Dihydroferulic acid 4-O-glucuronide
Urine 3-(3,5-dihydroxyphenyl)Propanoic acid
Urine Urolithin A-glucuronide
Urine Cholic acid
Urine Urolithin C
Faeces Chenodeoxycholic acid
Faeces Hyodeoxycholic acid
Faeces Deoxycholic acid
Faeces Leucine
Faeces Isoleucine
Urine Heptanoylcarnitine
Faeces Valine
Urine Indolelactic acid
Urine Phenylacetylglutamine
Urine Hippuric acid
Urine 5,6-Dihydroxyindole
Urine L-Kynurenine
Urine Methylcysteine sulfoxide
Urine Imidazolelactic acid
Urine Glucaric acid
Urine Hydroxyisovaleric acid
Urine Hydroxybutyric acid
Urine 3-hydroxy-L-tryptophan
Urine Pantothenic acid
Urine P-cresol sulfate
Blood P-cresol sulfate
MF0112_acetate to acetyl-CoA
MF0060_Beta-oxidation
MF0102_mucin degradation
MF0054_arabinose degradation
MF0033_cysteine degradation (mercaptopyruvate pathway)
MF0030_threonine degradation (formate pathway)
MF0031_threonine degradation (propanoate pathway)
MF0013_glutamate degradation (crotonyl-CoA pathway)
MF0070_galactonate degradation
MF0051_sucrose degradation (Actinobacteria)
MF0020_Entner-Doudoroff pathway (glucose/mannose)
MF0101_Sulfate reduction (assimilatory)
MF0111_triacylglycerol degradation
MF0057_alpha-D-glucose and alpha-D-glucose 1-phosphate degradation
MF0065_acetylneuraminate and N-acetyl-D-glucosamine degradation
MF0114_acetyl-CoA to crotonyl-CoA
MF0091_beta-D-glucuronide and D-glucuronate degradation
MF0027_cysteine degradation
MF0024_methionine degradation (propanoate pathway)
MF0001_ethanol production (formate pathway)
MF0056_galactose degradation (Leloir pathway)
MF0058_fructose degradation
MF0040_lysine degradation (cadaverine pathway)
SFA
ItMedIndex
PUFA
VP/AP
Vegetable Proteins (VP)
Dietary Fiber
Spearman Rho
1
0.5
0
-0.5
-1
MSP_Metabolites
MSP_GMM
MSP_Food

Supplementary Figure 30 Distinctive metabolites, dietary and microbial signatures between ConD and MedD diets at 4 weeks. Spearman correlations of contrasted MSP species with metabolites, GMM modules and nutrients at 4w. Rows, complete list of contrasted MSP at 4w between ConD and MedD diets ($p \leq 0.05$); Columns; contrasted annotated metabolites, contrasted GMM functional modules and nutrients data. Coloured-text referred to enrichment status (orange; ConD, green; MedD). Adjustments were performed using the Benjamini-Hochberg procedure and Spearman rho values were filtered by keeping correlations with at least one FDR≤0.05. Solid dot, FDR≤0.05; Open dot, FDR≤0.2.

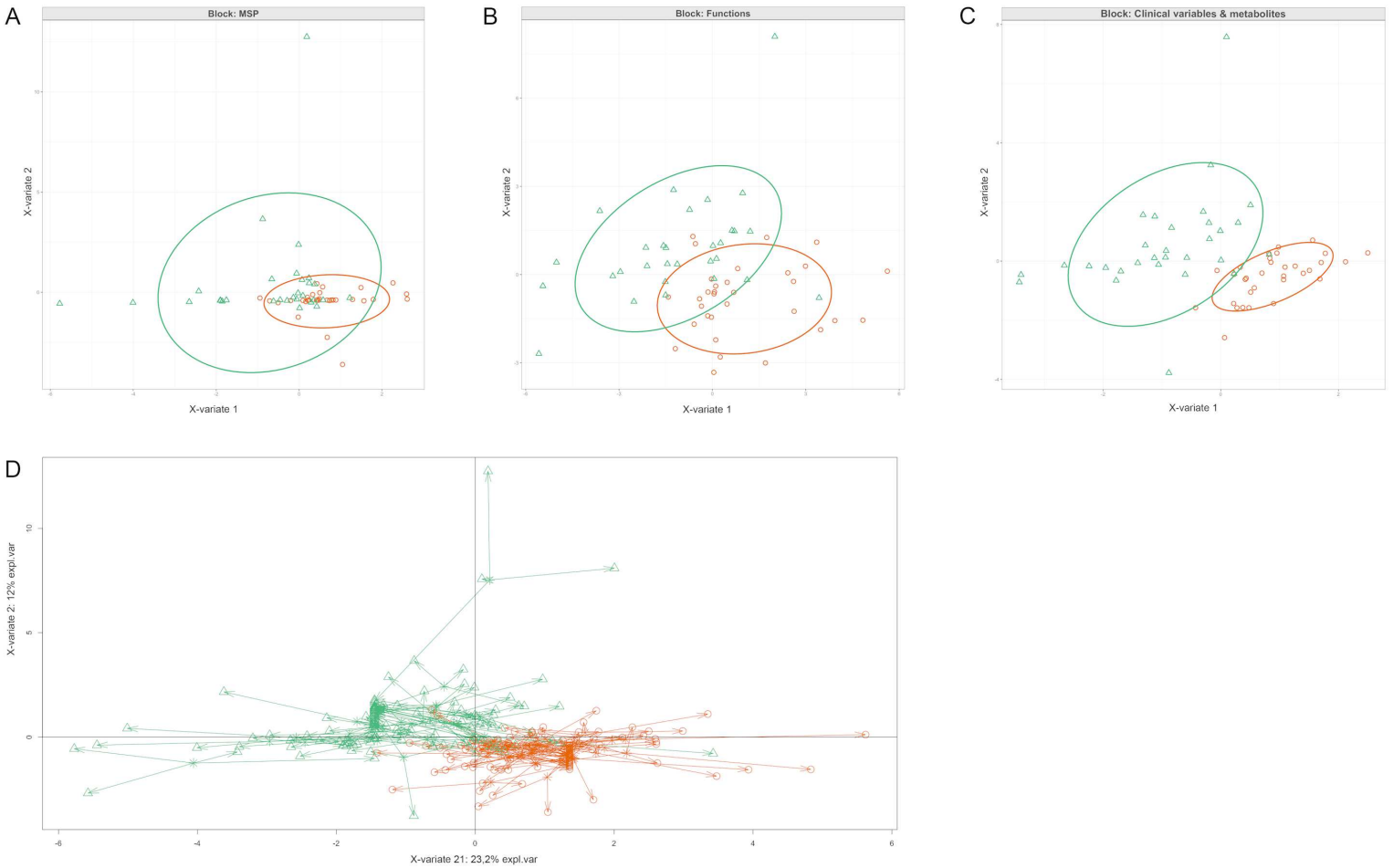

Supplementary Figure 31 N-integrative supervised analysis of different types of ‘omics datasets. The DIABLO model for the discrimination of ConD and MedD groups is displayed as sample plot per single ‘omic level. (A) Overall microbiota composition, (B) gut metabolic modules, (C)

clinical variables and metabolome single-omic levels are reported along with (D) co-inertia analysis quantifying the co-variability between the three multi-omics datasets. Shapes represent the projected coordinates of each subject. The centroid for a given sample between all ‘omics datasets is indicated by the start of the arrow and the location of the same sample in each dataset by the tips of the arrows. The length of the arrow is proportional to the divergence between data from different blocks. The percentage of total explained variance describing the separation of the groups on the first two components are displayed on the x and y axis, respectively. Green triangles, MedD subjects. Orange circles, ConD subjects. The integration of meta-omics products was associated with an increase in classification accuracies in discriminating between the ConD and MedD groups with respect to the cases in which a single data type was used. The AUC increased to 0.92 (from 0.88) when using metabolomics data only and to 0.90 (from 0.87) when comparing the ConD and MedD groups at 4 weeks and 8 weeks, respectively.

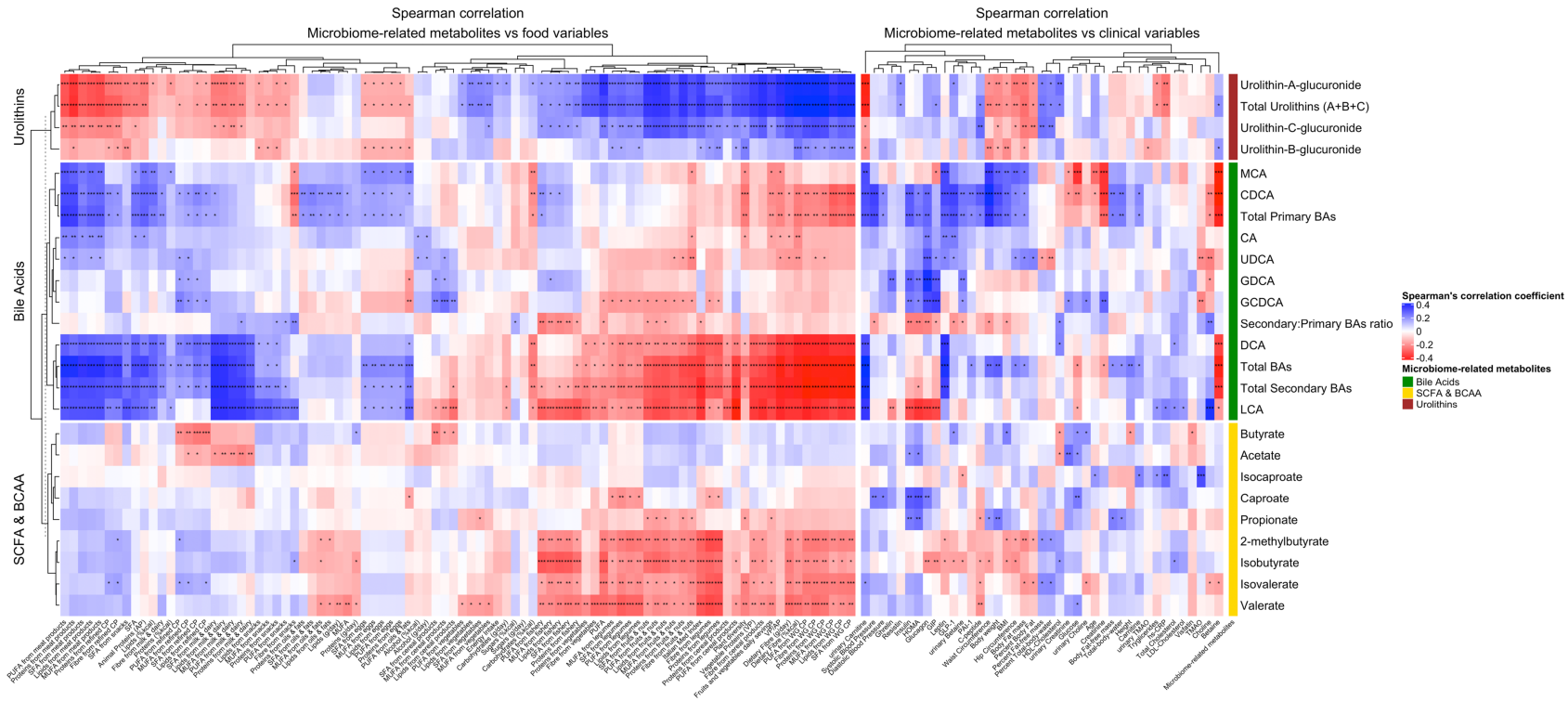

Supplementary Figure 32 Correlation of microbiome-related metabolites with dietary and clinical variables. Heatmap showing hierarchical Ward-linkage clustering of microbiome-related metabolites based on Spearman's correlation with dietary variables and clinical parameters. The colour scale represents the scaled version of Spearman's rho coefficients, with red indicating negative and blue indicating positive correlations. BAs, bile acids; CDCA, Chenodeoxycholic acid; MCA, Muricholic acid; DCA, Deoxycholic acid; GCDCA, Glycochenodeoxycholic acid; GDCA, Glychodeoxycholic acid; LCA, Lithocholic acid; UDCA, Ursodeoxycholic acid; SCFA, short-chain fatty acids; BCAA, branched-chain amino acids. TMAO, trimethylamine oxide; GLP-1, glucagon-like peptide-1; GIP, glucose-dependent insulinotropic peptide. VP/AP, Vegetable Protein/Animal Protein; PUFA, polyunsaturated fatty acid; MUFA, monounsaturated fatty acids; SFA, saturated fatty acids;WG, whole grain; CP, cereal products. Adjustments were performed using the the Benjamini-Hochberg procedure and Spearman rho values were filtered by keeping correlations with at least one FDR≤0.05. (*FDR<0.05, **FDR< 0.01 and ***FDR< 0.001).

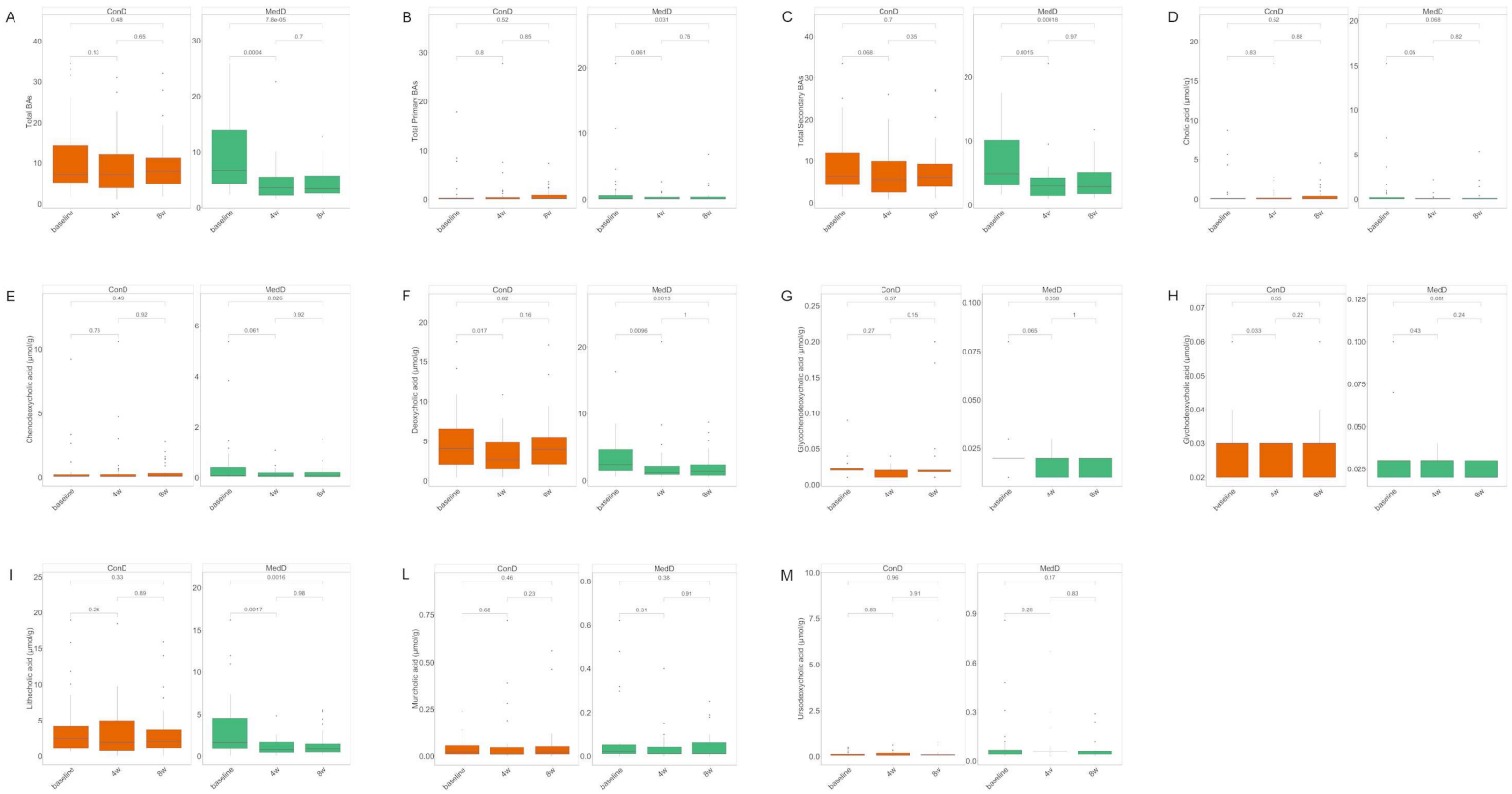

Supplementary Figure 33 Box plots showing faecal concentrations of several BAs measured throughout the intervention. (A) Total BAs, (B) Total primary BAs, (C) Total secondary BAs, (D) Cholic acid, (E) Chenodeoxycholic acid, (F) Deoxycholic acid, (G) Glycochenodeoxycholic acid, (H) Glychodeoxycholic acid, (I) Lithocholic acid and, (L) Muricholic acid, (M) Ursodeoxycholic acid. Orange indicates ConD while green colour refers to MedD subjects, respectively. P values indicate paired Wilcoxon rank-sum tests within each group. Baseline, 0 weeks; 4w, 4 weeks; 8w, 8 weeks of intervention.

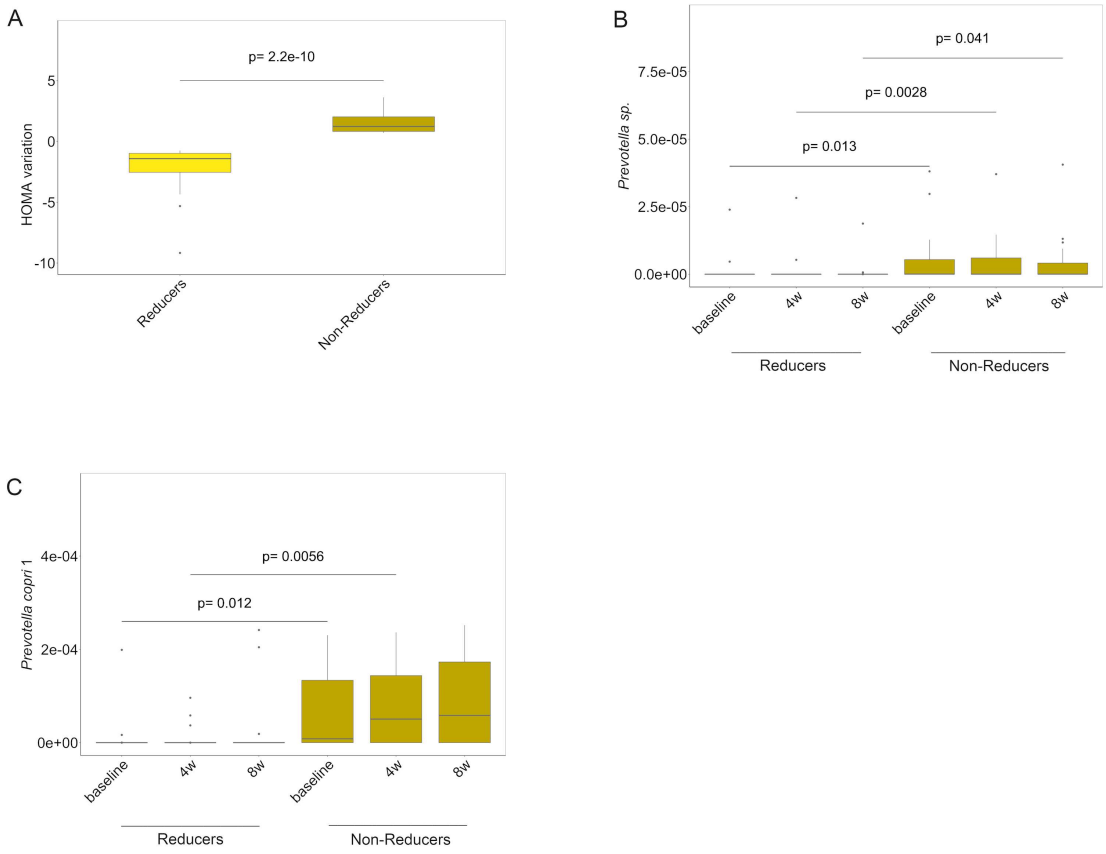

Supplementary Figure 34 Box plots showing differences in (A) HOMA variation classifying the subjects in HOMA reducers (Yellow) and non-reducers (Dark gold) after 4 weeks of intervention. Differences in levels of (B) *Prevotella* sp. and (C) *Prevotella copri* 1 in HOMA reducers and non-reducers. Statistical differences between groups were determined using unpaired Wilcoxon rank-sum tests. Baseline, 0 weeks; 4w, 4 weeks; 8w, 8 weeks of intervention.

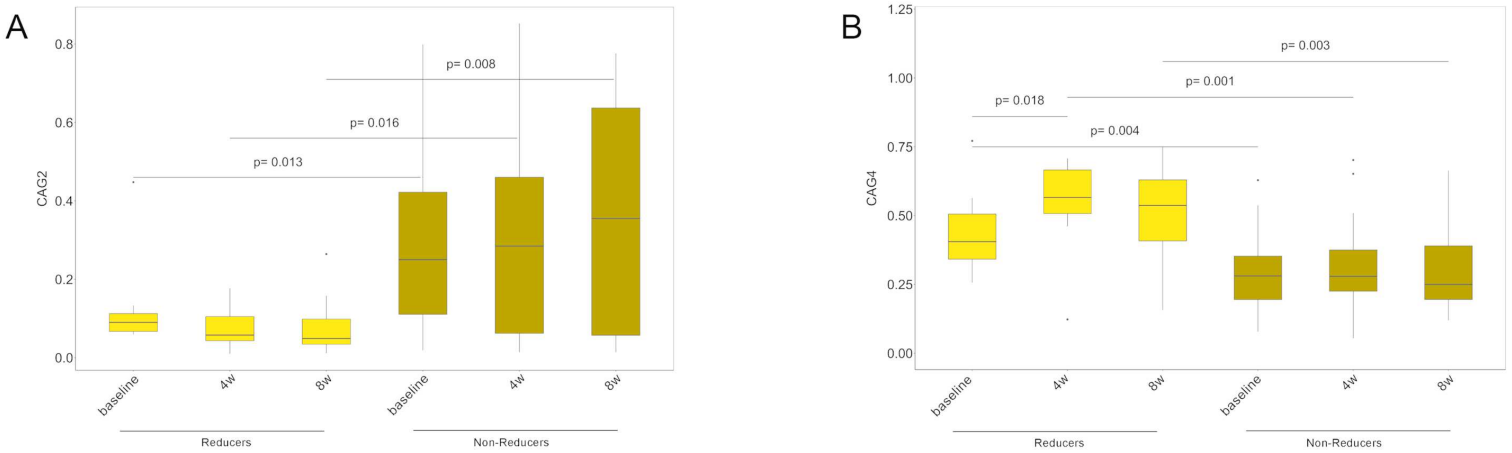

Supplementary Figure 35 Box plots showing differences in abundance of Co-Abundance Groups (CAGs) obtained from 16S rRNA gene sequences in subjects classified as HOMA reducers (Yellow) and non-reducers (Dark gold) after 4 weeks of intervention. Statistical differences between groups were determined using unpaired Wilcoxon rank-sum tests. Baseline, 0 weeks; 4w, 4 weeks; 8w, 8 weeks of intervention. Only (A) CAG2 and (B) CAG4 are reported, since no significant variation was found for the others.

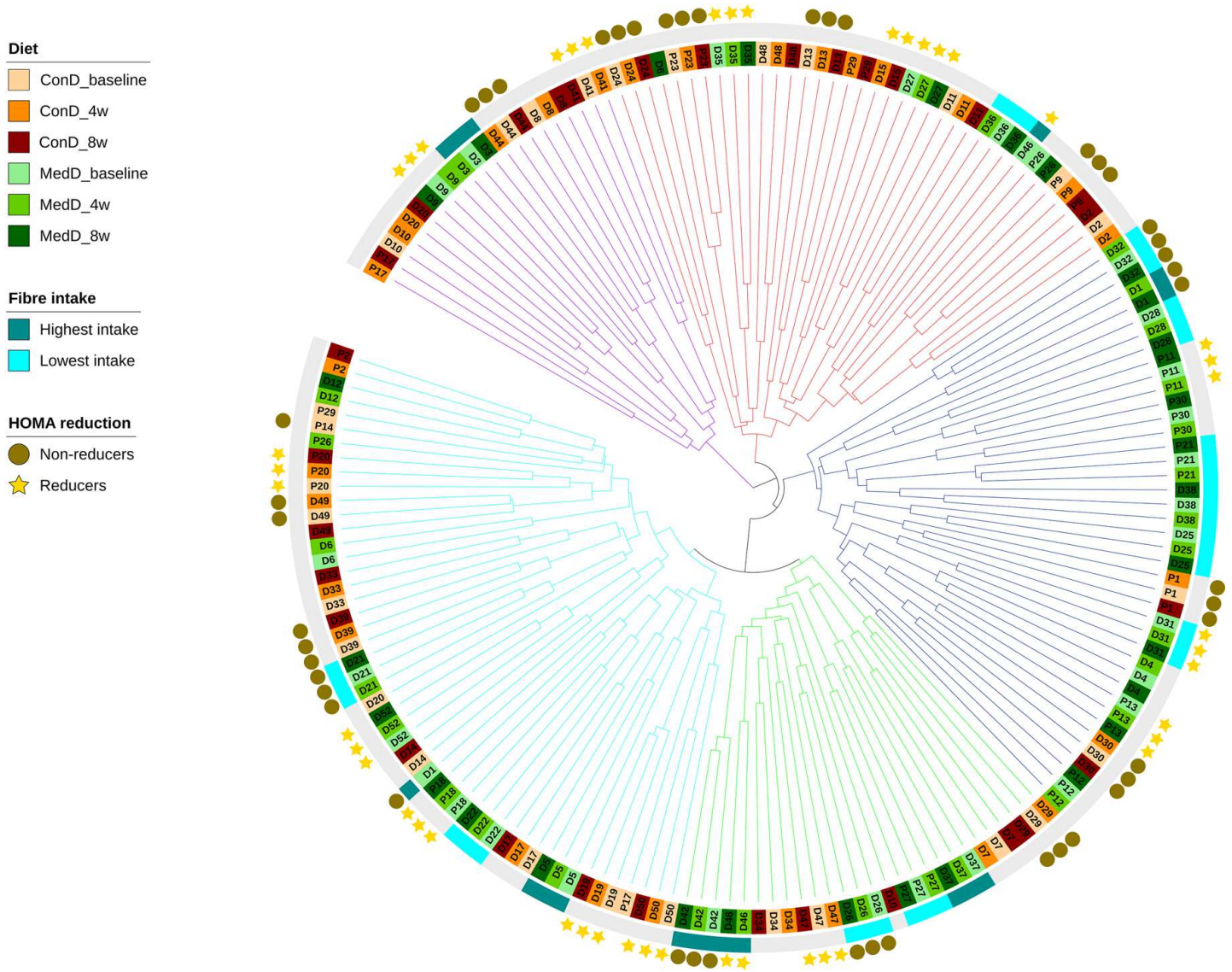
Diet
ConD_baseline
ConD_4w
ConD_8w
MedD_baseline
MedD_4w
MedD_8w
Fibre intake
Highest intake
Lowest intake
HOMA reduction
Non-reducers
Reducers

Supplementary Figure 36 Circular tree showing clustering of the subjects based on *Faecalibacterium prausnitzii* pangenome. Subjects are coloured according to dietary treatment and time-points. Coloured ring indicates the quartile of highest (green) versus lowest (cyan) increase of dietary fibre intake. Subjects not falling in the highest or lowest quartile were coloured in grey. Yellow stars or dark gold dots indicate HOMA reducers and non-reducers